The Impact of a Noise Mitigation Screen on the Scour Protection

Process identification and worst case evaluation

C.J. Baas

Delft University of Technology

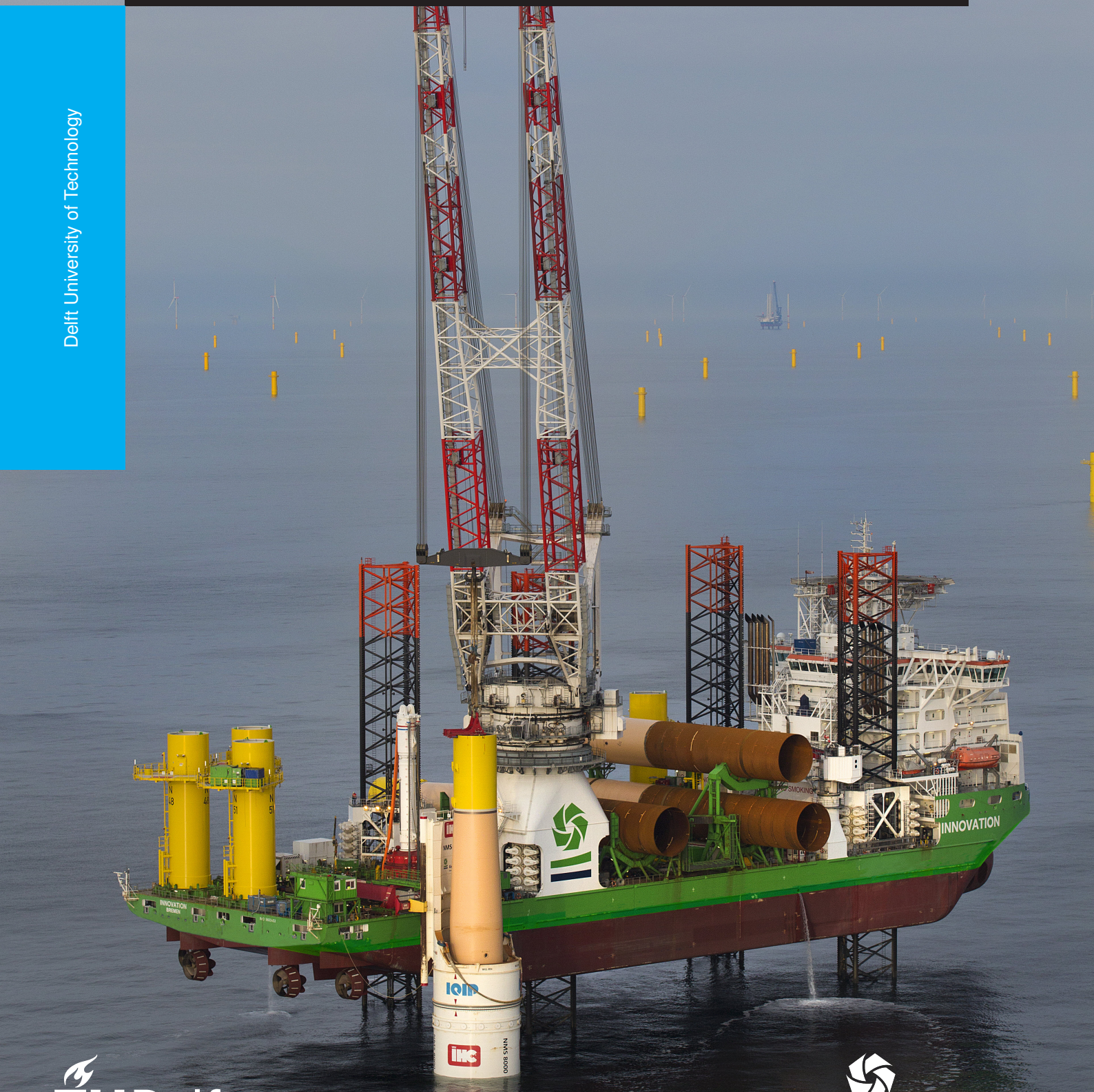

TU Delft

Tideway
Offshore Solutions

The Impact of a Noise Mitigation Screen on the Scour Protection

Process identification and worst case evaluation

by

C.J. Baas

to obtain the degree of Master of Science
at the Delft University of Technology,
to be defended publicly on Thursday July 12, 2018 at 14:30.

Student number:	4160525	
Project duration:	August 21, 2017 – July 12, 2018	
Thesis committee:	Prof.dr. A. Metrikine,	Chairman, TU Delft
	Ir. T.C. Raaijmakers,	Daily Supervisor, TU Delft
	Ir. C.W. Visser,	Supervisor, Tideway Offshore Solutions
	Ir. C. Lupea,	Daily Supervisor, Tideway Offshore Solutions
	Dr.ir. K.N. van Dalen	External committee, TU Delft

This thesis is confidential and cannot be made public until July 12, 2023.

TU Delft

Abstract

DELFT UNIVERSITY OF TECHNOLOGY
TIDEWAY OFFSHORE SOLUTIONS

Master of Science Offshore and Dredging Engineering
The Impact of a NMS on the Scour Protection
by C.J. Baas

Current trends show that the offshore wind industry is evolving into deeper waters, with larger turbines and consequently larger foundations. In Europe 80% of the wind turbines are installed on monopile foundations and this is expected to be the dominant choice in the future. The shallow geology of most of the wind farms is characterized as sand. A known phenomenon around foundations in sandy soils is the occurrence of scour, due to a disturbance in the flow caused by the waves and currents. Scour affects the embedment depth and natural frequency of the turbine. In order to prevent these effects a commonly used technique is to install a rock blanket around the monopile, to act as scour protection. Monopiles are mostly driven into the soil with a hydraulic impact hammer. The blows of the hammer result in an elevated noise level. Within the German EEZ strict rules are set regarding the allowable noise level. Noise mitigation measures, such as a noise mitigation screen, are used to prevent exceedance of the sound exposure level, see figure 1.

In an attempt to reduce the Levelised Costs of Energy (LCOE) of offshore wind, cost-saving optimizations are considered such as the installation of a single layer scour protection before foundation installation. The conventional two layer system requires two mobilization campaigns one for the filter and the second for the armour layer, after monopile installation. The single layer solution results in a reduced installation time and no risk of collision with the monopile. The NMS is lowered on the scour protection and the monopile is driven through the NMS. During the installation the NMS penetrates in the scour protection and deformations are observed, see the area close to the monopile in figure 1. Remedial works are very expensive and therefore one would like to know what the impact is on the performance of the scour protection during the lifetime of the wind farm.

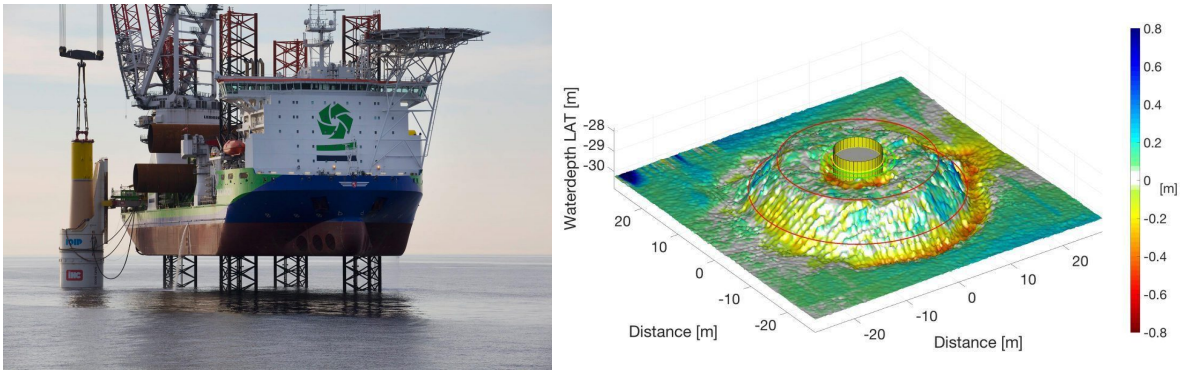

Figure 1: Left, monopile installation with NMS. Right, deformed scour protection by NMS

The project is based on a review of literature regarding relevant topics such as: soil mechanics, scour protection, noise mitigation and installation processes. Because of the problem's novelty, the available research is limited. In order to acquire insight in to the problem there is a need to investigate which processes are involved and relevant. This is done by collecting all available field data from selected offshore wind farms installed with a NMS, such as CPT data, survey data and hammer logs.

The analysis of the available data shows that the main factor influencing the NMS penetration is the combination of the use of a NMS together with the hammering procedure. Based on the available soil, hammer log, NMS and pile penetration data it is believed that the NMS imprint is a consequence of compaction of the underlying soils and scour protection. Compaction of underlaying soils is seen as having a beneficial effect on the scour protection system. Further it is investigated whether a large NMS penetration combined with a high relative mobility for the scour protection during storm conditions can lead to undesirable effects. Time series of environmental conditions were reconstructed from field measurements and numerical model hind casts. These time series serve as input to assess the relative rock mobility between installation and most recent bathymetry survey. Locations are verified for the imprint depth and relative mobility and a potential worst case is identified. The identified worst case is evaluated and validated against model tests of similar conditions. The outcome of the study is that limited rock movement has occurred from the edges of the imprint into it, but that the scour protection is still performing well after a 5yr design storm. This is also confirmed by model tests. A potential weak-link is identified in the slope of the imprint where the scour protection thickness is reduced. Practical mitigation and monitoring measures are proposed, but further research is needed to verify whether the risk of winnowing can appear within the slope of the deformed part of the imprint.

The results of this thesis are relevant for scour protection systems of monopile foundations installed on sandy seabeds, where impact pile driving and NMS are used. Limited available research has led to a qualitative empirical approach where the field results have been explained and back-quantified with known available theories.

The aim of the thesis has been achieved, it us observed that NMS penetrations are mostly influenced by the dynamics of the hammering process, resulting most likely in compaction of the underlying soils. Evaluating the worst case and validating against measured field data shows that the scour protection is still performing well according to the design requirements up to the past 5 year storm conditions. However there is a different deformation pattern observed which results in a shift in the critical spot for failure to occur in the scour protection.

Preface

I would like to thank Tideway Offshore Solutions for giving the opportunity to do my graduation thesis on a relevant topic for the industry nowadays. Specials thanks to my supervisors Ir. Connie Visser and Ir. Cristina Lupea for the support and willingness to help during my thesis. I would like to thank Ir. Sylvie Raymackers from GeoSea as well for the support and providing all the data in order to link the relevant activities from both DEME subsidiaries. Also many thanks to my colleagues in the engineering department of Tideway for the enjoyable time and interesting conversations. I also would like to thank Tideway Offshore Solutions and namely Bert Eversdijk for giving me the opportunity to start my career within the company and to gain more experience.

I would also like to thank my university supervisors, chairman of my graduation committee Prof. dr. Andrei Metrikine, for his critical comments and keeping me on track, and the PhD candidate Ir. Tim Raaijmakers for his support. I am very grateful to Tim Raaijmakers for our regular discussions and sharing his knowledge about scour protections which helped my to gain a better understanding of the problem and improve the level of my work.

Finally, I would like to express my gratitude to my friends and family for their support. Special thanks to my parents who made this possible and to my girlfriend who helped me through the hard times.

C.J. Baas
Delft, July 2018

Contents

List of Figures

List of Tables

Nomenclature

List of Abbreviations

AV	Alpha Ventus
CPT	Cone Penetration Test
$DEME$	Dredging, Environmental and Marine Engineering
$DP2$	Dynamic Positioning 2
EEZ	Exclusive Economic Zone
ELC	Extreme Load Case
ESA	Effective Stress Analysis
EU	European Union
$EWEA$	European Wind Energy Association
FEM	Finite Element Modelling
FoS	Factor of Safety
$FPROV$	Fallpipe Remote Operated Vehicle
FPV	Fallpipe Vessel
GPS	Global Positioning Sensor
HAT	Highest Astronomical Tide
HD	High Density
HSD	Hydro Sound Damper
HTU	Horizontal Transport Unit
ID	Inner Diameter
$IFPS$	Inclined Fallpipe System
KC	Keuligan-Carpenter
LAT	Lowest Astronomical Tide
MOB	Mobility Index
MP	Monopile
MPM	Material Point Method
MPV	Multi Purpose vessel
MWD	Mean Wave Direction
NCL	Normal Consolidation Line
NMS	Noise Mitigation System/Screen

$NS1$	Nordsee One
OCR	Overconsolidation Ratio
OD	Outer Diameter
OWF	Offshore Wind Farm
PSD	Particle Size Distribution
RES	Renewable Energy Resources
$RSDU$	Rock Side Dump Unit
SBT	Soil Behaviour Type
SDU	Stone Dumping Unit
TP	Transition Piece
TSA	Total Stress Analysis
URL	Unloading Reloading Line
WD	Waterdepth
WTG	Wind Turbine Generator

List of Symbols

α_{cw}	Angle between waves and currents	[°]
ϵ	Strain	[–]
γ	Unit weight	$[kN/m^3]$
$\hat{T}$	Natural period of the system	$[m/s^2]$
κ	Von Karman's constant	[–]
ν	Kinematic viscosity	$[m^2/s]$
ω	Wave frequency	$[rad/s]$
ϕ'	Friction angle	[°]
ρ	Density	$[kg/m^3]$
σ'	Effective stress	$[kPa]$
σ_{v0}	Initial total vertical stress	$[kPa]$
τ	Shear stress	$[kPa]$
τ_0	Bed shear stress	$[N/m^2]$
θ	Shields parameter	[–]
A	Orbital stroke	$[m]$
c	Cohesion	$[kPa]$
C_c	Compression index	[–]
C_d	Drag coefficient	[–]
C_r	Recompression index	[–]

d	Depth factor	$[-]$
D_*	Dimensionless grain size	$[-]$
D_r	Relative density	$[-]$
d_{50}	Median particle size	$m]$
d_{pile}	Diameter monopile	$[m]$
E	Young's modulus	$[kPa]$
e	Void ratio	$[-]$
F_r	Normalized friction ratio	$[-]$
f_w	Wave friction factor	$[-]$
g	Gravitational acceleration	$[m/s^2]$
H_s	Significant wave height	$[m]$
h_{total}	Total waterdepth	$[m]$
I_c	SBT Index	$[-]$
k	Permeability	$[m/s]$
k	Wave number	$[m^{-1}]$
K_f	Bulk modulus fluid	$[kPa]$
k_s	Nikuradse equivalent sand grains roughness	$[m]$
k_s	Roughness height	$[m]$
KC	Keuligan Carpenter number	$[-]$
L	Drainage length	$[m]$
L	Wavelength	$[m]$
MOB	Mobility index	$[-]$
N	Bearing capacity factor	$[-]$
n	Porosity	$[-]$
p_a	Atmospheric pressure	$[MPa]$
Q_t	Normalized cone penetration resistance	$[-]$
q_t	Cone resistance	$[MPa]$
r	Relative roughness	$[-]$
R_w	Wave Reynolds number	$[-]$
s	Shape factor	$[-]$
s_u	Undrained shear strength	$[kPa]$
T	Imposed period	$[s]$
T_p	Peak period	$[s]$
u	Pore water pressure	$[kPa]$

U_w	Amplitude wave orbital motion	$[m/s]$
u_*	Friction velocity	$[m/s]$
U_c	Depth-averaged current velocity	$[m/s]$
U_{rel}	Relative velocity	$[-]$
V_c	Compression wave velocity	$[m/s]$
z_0	Bed roughness length	$[m]$

Chapter 1

Introduction

1.1. Background

Renewable Energy Sources (RES) contribute to climate change mitigation by lowering the greenhouse gas emissions, achieve sustainable development, taking care of the environment and improve human health. Renewable energy is also an emerging stimulus for economic growth, creating jobs and reinforcing energy security across Europe.

The Europian Union (EU) wants to be the worldwide leader in promotion and development of renewable energy. By 2020, 20% of the total energy consumption in Europe should be renewable, this is published in [European Commission, 2009]. In 2016 the directive was updated with a new target, By 2030 27% of all energy consumed in the EU should originate from renewables [European Parliament and the Council, 2016].

Wind energy plays a major role in reaching the goals stated above. Wind is the fastest growing energy source in the world and a crucial part of Europe's industrial base. In Europe the wind sector represents over 300,000 jobs, generates €72 billion in annual turnover and has a 40% share of all wind turbines sold globally. Begin 2017 the share of wind energy is 10.4% of Europe's total energy consumption with the capacity installed (153.7 GW) [WindEurope, 2017b].

Offshore wind went through a large development the last decade, see figure 1.1. The installed capacity offshore amounts of 12.6 GW begin 2017, this is about 1/12 of the total renewable wind energy production and is expected to extend to 24.6 GW by 2020 [Wind Europe, 2017]. The European Wind Energy Association (EWEA) even has a central scenario for 2030 with an installed offshore wind capacity of 66.6 GW [EWEA, 2015]. A more recent study by Wind Europe has investigated the potential of offshore wind in Europe, taking into account wind speeds, water depths, shipping lanes, technology, marine protected area's etc. They stated that in 2030 in the base scenario a cumulative total offshore capacity of 64 GW is installed in Europe. This will be 7% - 11% of the EU's electricity demand [WindEurope, 2017a]. So the coming years offshore wind will become about 5 times as large compared to begin 2017.

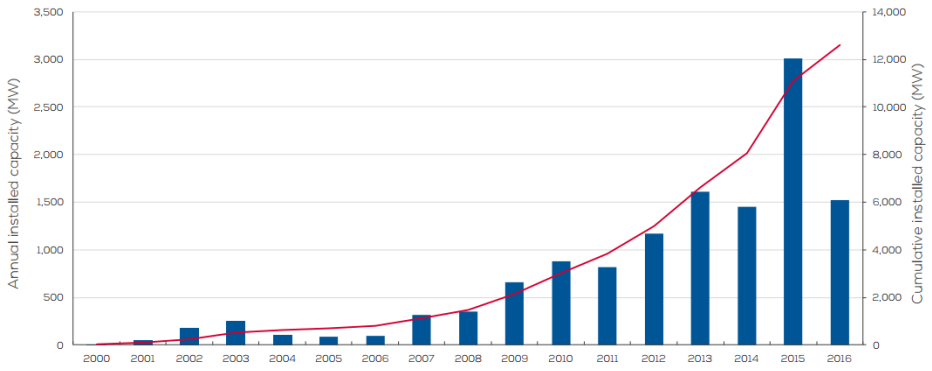

Figure 1.1: Annual and Cumulative installed capacity Offshore Wind Turbines
Source: WindEurope - 2016

Current offshore wind farms are commercially attractive in shallow waters with water depths up to 40m-50m [Europe, 2013]. The wind turbines are often installed on a pre-installed substructure (foundation), see figure 1.2. Begin 2017 in Europe 3589 offshore wind turbines are installed, 81% of substructures are monopiles, 7.5% are gravity foundations, jackets account for 6.6%, tripods account for 3.2% and tripiles account for 1.9% [Wind Europe, 2017].

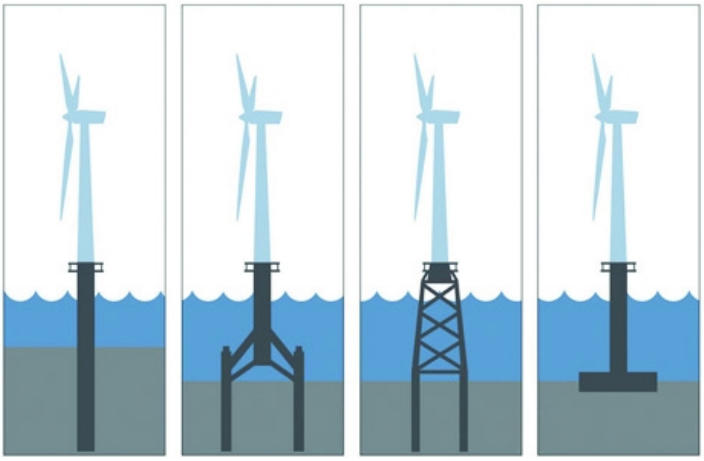

Figure 1.2: Offshore wind turbine foundation types for shallow water. In Europe 3589 offshore wind turbines are installed, 81% of substructures are monopiles, 7.5% are gravity foundations, jackets account for 6.6%, tripods account for 3.2% and tripiles account for 1.9% [Wind Europe, 2017]
Source: The Engineer

Current trends show that wind turbines are getting bigger and are installed in deeper waters. This brings a lot of new technical challenges, also for the foundation. Monopiles will still remain the dominant structure because of the speed of the fabrication process and the ease of transportation compared to, for example, jackets [Fischer, 2015]. As an example, in the United Kingdom the Hornsea One offshore wind farm owned by Ørsted is in the (pre)-construction phase (end 2017). The project consists of 7 MW wind turbines connected to monopiles with a diameter up to 8.1m and a weight of 900 tons. All the 174 wind turbines will be installed in waterdepths up to 37m by DEME.

A known phenomenon in sandy/silty seabed is the occurrence of local scour around monopiles. The monopile disturbs the flow caused by the waves and currents. creating a down flow in front of the monopile and a horseshoe vortex near the seabed. Sand particles are picked up by the fast flowing water creating a hole around the monopile. Scour has a negative influence on the foundation embedment depth and the natural frequency of the monopile [van der Tempel et al., 2004]. One could allow the scour to develop and take it into account for the structural design or protect the seabed against scour. In order to protect the seabed against scour, one need to reduce the current velocities in the vicinity of the structure to reduce the scour effect. This can be done with for example the use of artificial seaweed fronds creating an unbroken viscous drag layer above the seabed. A study performed, shows that the artificial seaweed reduces the flow 0.1m above the seabed to 72% in constant flow and 92% in variable flow [Jones et al., 2003]. The main engineering problem is to provide adequate anchorage of the system to the seabed. A more common used technique is to place a rock blanket around the monopile, so called scour protection. To prevent the sand particles washing out of the rocks also bij affecting the flow conditons. Scour protection often consists of one or two layers with different rock gradings.

Tideway Offshore Solutions, a subsidiary the Belgian group Dredging, Environmental and Marine Engineering (DEME), has a vast experience in installing these scour protections. Tideway currently operates three Dynamic Positioning 2 (DP2) fallpipe vessels, “Seahorse” (17,000 t), “Rollingstone” (11,500 t) and the Ice Class vessel “Flintstone” (17,500 t). Summer 2018 the new DP3 Multi Purpose Vessel (MPV) vessel “Living Stone” will be ready for employment. Together with “GeoSea”, another subsidiary from DEME specialized in Installation & Decommissioning and Foundation works, Tideway completes a lot of offshore wind farm projects. GeoSea installs the monopile and transition pieces while Tideway equips them with a proper scour protection. The Inclined Fallpipe System (IFPS) and Rock Side Dump Unit

(RSDU) are used for rock placement close to monopiles and placement of larger gradings of rock. For filter layers or single layer systems which consist of smaller gradings the conventional fallpipe system will be used.

Monopile installation with impact hammers produces noise and has a certain impact on the marine environment. In Europe the instances are aware of it but have not come to an overall agreement yet. Germany is known for having the strictest requirements with respect to piling noise levels. The impact of noise from piling activities on marine mammals, particularly harbor porpoises (Phocoena phocoena), has become a crucial aspect in the process of approving windfarm projects in German waters. The federal law on nature protection has stated that it is forbidden to injure or significantly disturb the harbor porpoises. This has lead to noise mitigation regulations in the German Exclusive Economic Zone (EEZ). The following measure was formulated with in the 'Noise mitigation concept' (2013) by the Federal Ministry for the Environment (BMU): Threshold levels 160dB re μPa SEL and 190dB re μPa L_{peak} in 750m distance to the piling location [BSH, 2011]. These regulations have lead to development of Noise Mitigation Systems (NMS) for reducing the piling noise. Examples of different noise mitigation measures can be seen in figure 1.3. These examples will be explained in section 2.3.

(a) GeoSea vessel Innovation installation with NMS and bubble curtain on Gode Wind OWF

(b) GeoSea vessel Innovation monopile installation with IHC NMS-8000

Figure 1.3: Different Noise Mitigation Systems in use
Source: GeoSea

Installation of the foundations for an offshore wind farm consists of 20-25% of the total costs. Therefore contractors and subcontractors are continuously searching for possibilities to reduce these cost. A new trend within the installation of scour protection is to install a single layer scour protection before the monopiles are installed. In this case they have one single campaign to execute in order to save time. The common way to do this used to be first installing a filter layer, install the monopile through the filter layer and afterwards place an armour layer on top of the filter. Tideway has to assure the client that the agreed quantities and design have been met. On board of the rock placement vessels survey equipment is installed to pre- intermediate- and post survey of the installed scour protection at each monopile location to assure a proper scour protection design is installed. In case the rock berms do not meet the design requirements, remedial work has to be executed. When a filter and armour have to be installed, the remedial work can be done before installing the armour layer because the work that needs to be done is in the same offshore wind farm. The problem gets bigger when a single layer scour protection is applied. The monopile is installed through the scour protection, when the rock placement vessel might already be on another project. To reduce the noise a proven and common used concept is a Noise Mitigation Screen (NMS) developed by IHC in the German EEZ. The screen is lowered on the scour protection and the monopile is piled within the confinement of the NMS through the scour protection. However deformations to the scour protection are observed after installation. The question arises if the deformations need repairs which would result in high costs.

1.2. Operational Problem Identification

Tideway and GeoSea encountered some challenges during installation of the foundations for the offshore windfarms Merkur, Nordsee One, Gode Wind and Borkum Riffgrund. After the monopile was installed and the NMS was removed survey data revealed some remarkable aspects, see figure 1.4. It can be seen that for this location penetration of 0.60m occurred within the confinement of the NMS (green lines). Another remarkable aspect is that additional penetration seems to occur at the moment piling starts. The interaction of the NMS with the scour protection and the piling process is not yet understood. Also for the upcoming projects Hohe See, Albatros and Mermaid Seastar, challenges are expected with penetration of the NMS into the scour protection. From the mulitibeam surveys only elevations can be obtained, this means that there is no ability to look into the layers of the scour protection and soil. However a lot of different processes can occur during installation. In figure 1.5 several hypotheses for the interaction between NMS, scour protection and seabed during the installation process are illustrated. Depending on the actually occurred process, the future performance of the scour protection may be compromised. Compaction of the rock leads to a better filter working principle against winnowing but the layer thickness will be reduced 1.5b. If the soil underneath the scour protection compacts, the thickness of the scour protection remains the same and is unaffected 1.5c. In case the soil and rock mix up, the flow can easily reach the sand for winnowing because of reduction in effective thickness 1.5d. For figure 1.5e and f, the compaction of the rocks will have a positive effect but the mixing will lead to a reduction in performance. Another possibility is that the soil fails by lack of bearing capacity. So in order to evaluate the performance of the scour protection after installation it is important to know the root cause of the penetration and the influence to the scour protection. Factors which contain parameters that probably will have a relation or influence the penetration are assumed to be:

- Soil
- Scour Protection
- Noise mitigation
- Installation process

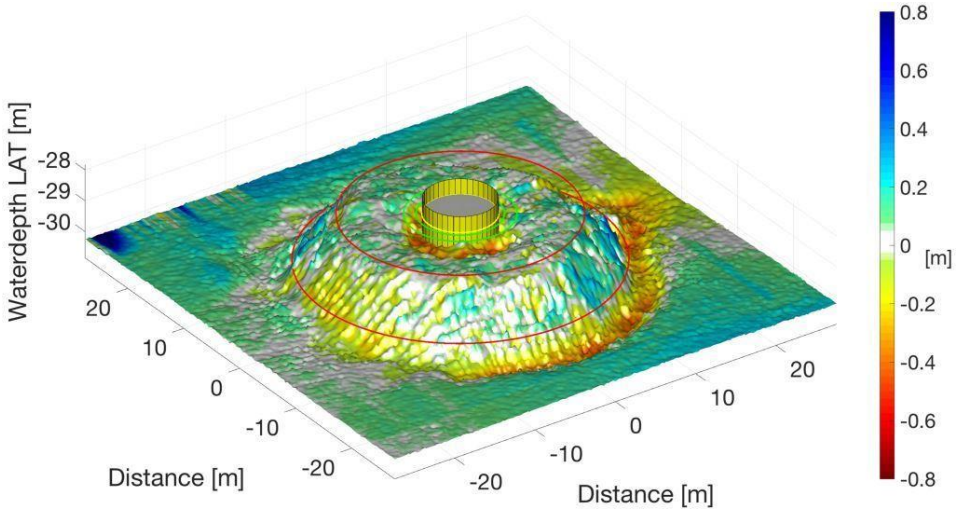

Figure 1.4: Scour protection deformation after monopile installation with NMS

The description of the problem results in the following **problem statement**
The use of a noise mitigation screen (NMS) when installing monopiles by impact pile driving, can lead to deformations of the scour protection which can affect the performance in some offshore wind turbine locations. At present, it is not known whether this deformation has a positive or negative effect on the performance on the scour protection.

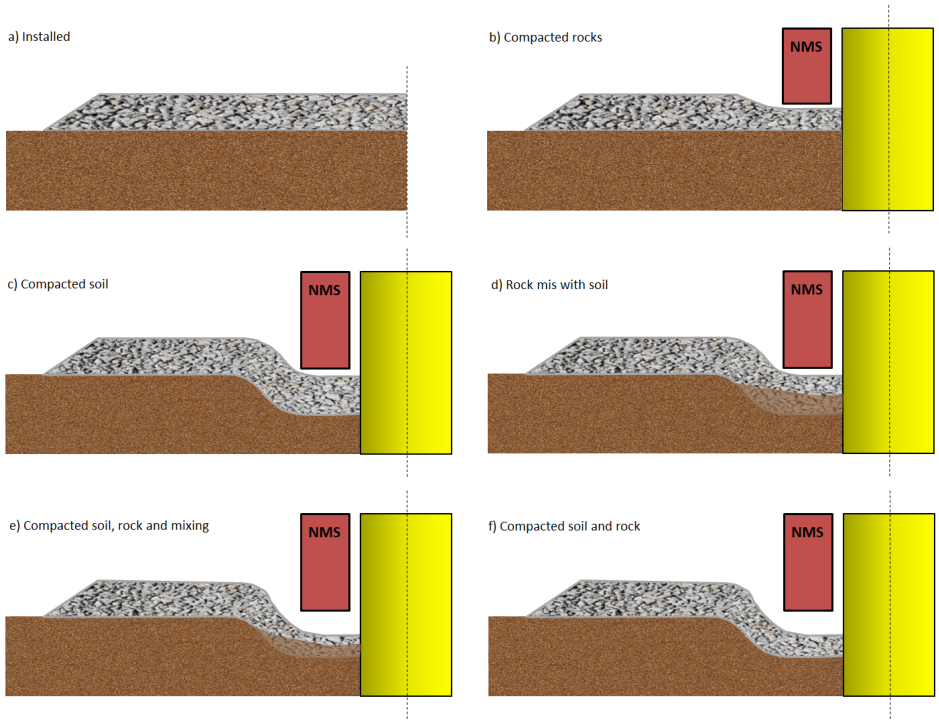

Figure 1.5: Cross sections for the different hypotheses for the interaction between NMS, scour protection and seabed during the installation process

The problem is known in the industry but not understood. To get a better understanding of the problem statement, the following main research questions rise:

- *Which processes and factors influence the Scour Protection deformations?*
- *What is the worst case scenario?*
- *Does the scour protection in the worst case still fulfill its purpose?*

1.3. The Practical Application and Aim of this thesis

The aim of this thesis is to first do a process identification analysis based on the available data. Out of this analysis the main factors that cause impact of the NMS on the scour protection follow. Together with the findings, the worst case scenario is investigated for one project. This scenario is subjected to functioning of the scour protection by comparing it to model tests. By doing this comparison the findings are validated and a better insight into the need of applying mitigation measures is known.

1.4. Thesis Approach

The approach to tackle the problem described in the problem statement can be subdivided into different parts. The first part is the literature study, this is necessary to get a better general understanding of the problem. Because of the problem's novelty limited research is available. Therefore there is a need to see which processes are involved and relevant for the problem. This is done by collecting all available field data from OWF's installed with a NMS, such as CPT data, survey data and hammer logs. All data should be analyzed that conclusions can be drawn. By doing this, the different processes which are relevant can be investigated. Attention is given to possible measurement errors. When all the data is processed, it is important to investigate what the worst case is with respect to the scour protection. Determining the worst case result in no need to look at other cases if the worst case still performs well and results in a better insight into the impact of the deformations. The last part consist of an evaluation of the worst case scenario based on model tests. Out of this comparison it is identified if the scour protection still will fulfill its function or if repairs are necessary. In case repairs are necessary, a discussion is needed about possible mitigation measures.

1.5. Thesis Outline

This thesis report compromises out of 6 chapters and is organized as stated below. In figure 1.6, a schematization of the content for each chapter is given with the corresponding relations between the different aspects.

Chapter 1 gives a background to the research together with the problem, practical application and target of this thesis.

Chapter 2 gives information and theory in order to get a better understanding to the problem. This chapter contains theory about soils, scour protection, noise mitigation and installation process.

Chapter 3 summarizes the project specifications for the projects which were installed with a NMS. Soils are investigated based on CPT interpretations, and a bearing capacity check is done and compared to the NMS penetrations. Also 3D visualizations are made in order to see the effect of difference in scour protection design and a comparison is made for an OWF which was installed without a NMS in order to see the influence. Since the available data sets for Merkur were most complete and this windfarm experienced significant NMS imprints, it was decided to further zoom in on this wind farm. Additionally, the NMS penetration logs are compared with the hammer logs and for the soil the liquefaction potential is investigated to gain more knowledge about the soil behavior.

Chapter 4 contains the formulation on what is understood as the worst case. Mobility calculations are performed based on the installed rock gradings together with the Metocean data since installation.

Chapter 5 contains the evaluation of the worst case. First the worst case is investigated in more detail. The worst case is compared to model tests performed during the design of the Merkur OWF. Monitoring seabed surveys are analyzed to compare the deformations observed in the field with the deformations during the model tests. The performance of the scour protection with NMS imprint is assessed based on this comparison.

Chapter 6 summarizes the conclusions made throughout this thesis and provides recommendations for further research and practical applications.

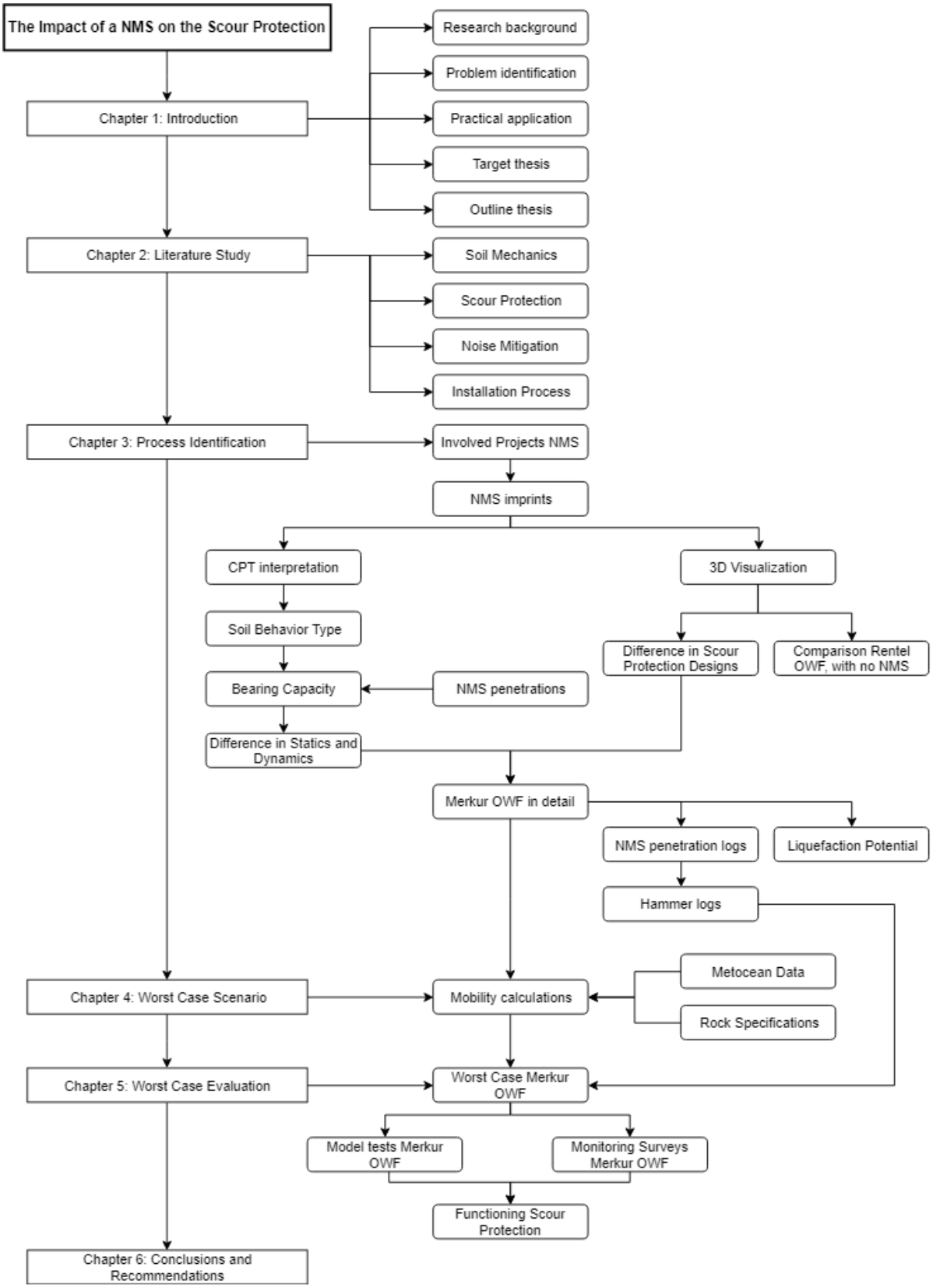

Figure 1.6: Schematization Thesis

Chapter 2

Literature Study

This chapter contains a review of literature regarding relevant topics such as: soil mechanics, scour protection, noise mitigation and installation processes. Because of the problem's novelty, the available research is limited. However with this review of literature a broader view is given for the involved aspects. This Result in a better understanding to the problem.

2.1. Soil Mechanics

2.1.1. Effective Stress

The principle of effective stresses is fundamental for soil mechanics. Deformations of soils are a function of effective stresses not total stresses. The principle of effective stresses applies only to normal stresses and not to shear stresses.

If an element of saturated soil is subjected to a normal stress (σ), applied to an horizontal boundary, then σ is called the total stress. According to Newton's third law the stresses in the soil must be equal and opposite to the total stress (given an equal unity area). The counter force to σ is provided by a combination of stresses. The stresses caused by the soil particles, so called effective stress σ'. And a stress caused by water in the pores, the pore water pressure u.

$$\sigma = \sigma' + u \tag{2.1}$$

So the effective stress is negatively affected by the pore pressure as follows:

$$\sigma' = \sigma - u \tag{2.2}$$

It is important to keep the following things in mind. The pore water cannot sustain shear stresses and therefore the soil particles must resist the shear forces, $\tau = \tau'$. Soils are not capable of handling tension forces. Which means the the effective stress can not be less than zero. In this report we use the sign conventions according to soil mechanics theory. This means compression will be positive(+) and tension will be negative(-).

2.1.2. One Dimensional Settlement Theory

Settlement of a soil occurs if a soil is loaded. A structure or foundation can settle uniformly or non uniformly. Nonuniform settlement is called differential settlement and is caused by the difference in soil layers and properties or nonuniform loads. The total settlement can usually be described in three different phases: Immediate or elastic compression (S_i), primary consolidation (S_c) and secondary compression (S_s). So that the total settlement $S_t = S_c + S_i + S_s$. In general for a normally consolidated fine grained soil, consolidation settlement is dominant. While for a normally consolidated coarse grained soil limited settlement occurs over time.

Elastic compression uses the principle of Hooke's law and makes the assumption that soil behaves elastically so that the soil will return to their original configuration after unloading. Primary consolidation is the change in volume of the soil caused by the expulsion of water from the voids and the transfer of load from the excess pore water pressure to the soil particles. Where the excess pore water pressure is the pressure in the pores after applying a load minus the current equilibrium pore water pressure, $\Delta u = u_1 - u_0$. Secondary compression is the change in volume of a fine grained soil caused by the

adjustment of the internal structure of the soil after primary consolidation has been completed. However in reality primary consolidation and secondary compression have no clear distinction. The rate of consolidation for a homogeneous soil depends on the permeability, thickness and length of the drainage path. According the principle of effective stress any reduction of the initial pore water pressure will be balanced by an increase in effective stress. Increase in vertical effective stress leads to soil settlement caused by changes in the soil structure. After a longer time the excess pore water pressure becomes zero because of the dissipation process and the volume decrease becomes very small. At the end the applied vertical stress is transferred to the soil and the vertical effective stress becomes equal to the total stress.

The initial specific volume of a soil is $V = 1 + e_0$, with e_0 the initial void ratio. The change in volume is equal to the change in void ratio. For 1D consolidation, the volumetric strain $\epsilon_p = \epsilon_z$ so that:

$$\epsilon_z = \frac{\Delta z}{H_0} = \frac{\Delta e}{1 + e_0} \tag{2.3}$$

With H_0 the initial soil height, so the the primary consolidation settlement is:

$$\rho_{pc} = \Delta z = H_0 \frac{\Delta e}{1 + e_0} \tag{2.4}$$

The new void ratio at the end of the consolidation under a given load is:

$$e = e_0 - \Delta e = e_0 - \frac{\Delta z}{H_0}(1 + e_0) \tag{2.5}$$

The behaviour of the soil under different loads or load increments is displayed in figure 2.1a and b, a graph of the void ratio versus the vertical effective stress is shown. In figure 2.1c an arithmetic graph of the vertical strain (ϵ_z) versus the vertical effective stress is given.

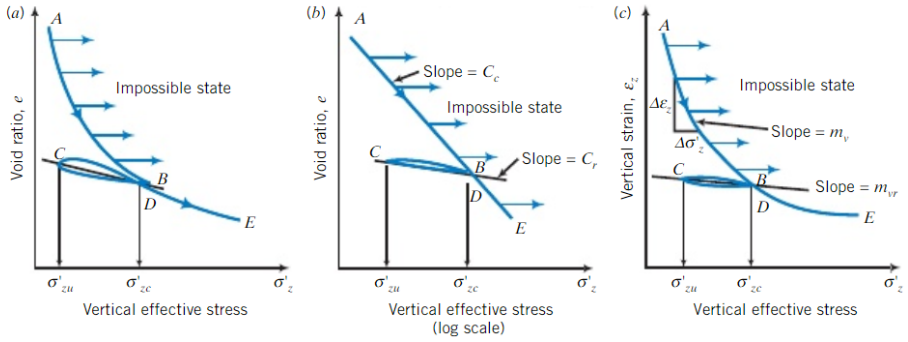

Figure 2.1: Three graphs of settlement data from soil consolidation
Source: Muni Budhi - Soil Mechanics and Foundations (2007)

Note that each increment of loading brings the soil into a denser state so that the soil permeability decreases. Therefore doubling the load from a previous increment, would not cause a double increase in settlement (No linearity). The line segment AB is called the virgin consolidation line or normal consolidation line (NCL), on logarithmic scale this line is approximately straight. At point B the soil is unloaded incrementally. When a part of the load is removed, relaxation occurs. The void ratio increases a bit but much less than the decrease of in void ratio for the loading that was first applied. The path BCD is the unloading and reloading of the soil, which can be averaged as the unloading reloading line (URL). Soil can be considered as an elastoplastic material. The line AB represents the elastoplastic response and BC the elastic response. In case the maximum vertical stress σ'_{zc} is exceeded the soil will follow the path DE which is the same as AB.

This is of major importance because every soil has its own loading history. The soil memorizes the past maximum effective stress. In case of placing a heavy structure such as a NMS on the soil the settlement would be small if the vertical effective stress does not exceed the past maximum vertical effective stress. In case it does exceed the past maximum stress significantly permanent settlement would occur. In

conclusion we can state that stresses below the preconsolidation stress, the soil will follow the URL and the soil behaves elastically. In case stresses are larger than the preconsolidation stress, the soil behaves like an elastoplastic material.

Figure 2.1 contains some important primary consolidation parameters. First the slopes of the NCL (coefficient of compression or compression index, C_c) and URL recompression index C_r are calculated as follows:

$$C_c = \frac{|\Delta e|}{log\left(\frac{\sigma'_{z,2}}{\sigma'_{z,1}}\right)} \tag{2.6}$$

$$C_r = \frac{|\Delta e_{zr}|}{log\left(\frac{\sigma'_{z,2}}{\sigma'_{z,1}}\right)} \tag{2.7}$$

The other parameter is respectively the modulus of volume compressibility (m_v) and the modulus of recompressibility (m_r)

$$m_v = -\frac{\epsilon_{z,2} - \epsilon_{z,1}}{\sigma'_{z,2} - \sigma'_{z,1}} = \frac{|\epsilon_z|}{\sigma'_{z,2} - \sigma'_{z,1}} \tag{2.8}$$

$$m_v r = -\frac{\epsilon_{z,2} - \epsilon_{z,1}}{\sigma'_{z,2} - \sigma'_{z,1}} = \frac{|\epsilon_{zr}|}{\Delta\sigma'_z} \tag{2.9}$$

The soil can be categorized based on their consolidation history. An overconsolidated soil is a soil which current vertical effective stress or overburden effective stress, σ'_{zo}, is less than its past maximum vertical effective stress or preconsolidation stress, σ'_{zc}. The degree of overconsolidation is expressed in the overconsolidation rate (OCR), which is defined as:

$$OCR = \frac{\sigma'_{zc}}{\sigma'_{zo}} \tag{2.10}$$

In case OCR = 1, the soil is normally consolidated.

Primary consolidation settlement can be subdivided into two parts. The normally consolidated soils and the overconsolidated soils. In the case of a normally consolidated soil placement of for example a NMS on the soil will increase the vertical stress at a depth z, $\Delta\sigma_z$. The final vertical stress will be:

$$\sigma'_{fin} = \sigma'_{zo} + \Delta\sigma_z \tag{2.11}$$

with the current vertical stress and change in vertical stress for a uniformly loaded cylindrical surface with radius r_0:

$$\sigma'_{zo} = (\gamma_{sat} - \gamma_w)z = \gamma' z \tag{2.12}$$

$$\Delta\sigma_z = q_S\left[1 - \left(\frac{1}{1 + (r_0/z)^2}\right)^{1.5}\right] \tag{2.13}$$

Due to the increase in vertical stress, the soil will settle following the NCL and the primary consolidation settlement will be:

$$\rho_{pc} = H_0\frac{\Delta e}{1 + e_0} = \frac{H_0}{1 + e_0}C_c log\frac{\sigma'_{fin}}{\sigma'_z o} \tag{2.14}$$

For the overconsolidated soils, two cases need to be considered depending of the magnitude of $\Delta\sigma_z$. In the first case the final effective stress keeps below the effective consolidation stress, $\sigma'_{fin} < \sigma'_{zc}$. Consolidation occurs along the URL:

$$\rho_{pc} = \frac{H_0}{1 + e_0}C_r log\frac{\sigma'_{fin}}{\sigma'_{zc}} \tag{2.15}$$

The other case is if $\sigma'_{fin} > \sigma'_{zc}$. Here two settlement components need to be considered. The first part of settlement follows the URL and the second part follows the NCL. This results in:

$$\rho_{pc} = \frac{H_0}{1+e_0}\left(C_r log\frac{\sigma'_{zc}}{\sigma'_{zo}} + C_c log\frac{\sigma'_{fin}}{\sigma'_{zc}}\right) = \frac{H_0}{1+e_0}\left(C_r log(OCR) + C_c log\frac{\sigma'_{fin}}{\sigma'_{zc}}\right) \tag{2.16}$$

Therefore the following procedure to calculate the primary consolidation settlement can be used:

1. Calculate the current vertical effective stress (σ'_{zo}) and void ratio (e_0) at the center of the soil layer.
2. Calculate the applied vertical stress increase ($\Delta\sigma_z$) at the center of the soil layer.
3. Calculate the final vertical effective stress (σ'_{fin})
4. Calculate the primary consolidation settlement (ρ_{pc}) depending on the normal- or overconsolidated soil.

Better accuracy is reached when dealing with thick soil layers ($H_0 > 2m$), to divide the soil in different sublayers and repeat the above calculations for the settlement of each sublayer.

After primary consolidation is finished, secondary compression takes part with a constant vertical effective stress. Secondary compression is less significant and a much slower process, see figure 2.2. The intersection of the tangent lines of the primary consolidation and secondary compression are denoted with t_p. The slope if the secondary compression line is the secondary compression index:

$$C_\alpha = -\frac{e_t - e_p}{log(t/t_p)} = \frac{|\Delta e|}{log(t/t_p)} \quad , \quad t > t_p \tag{2.17}$$

Secondary compression is of main interest in normally consolidated soils, in overconsolidated soils secondary compression or creep is not significant. The secondary settlement can be calculated:

$$\rho_{sc} = \frac{H_0}{1+e_p} C_\alpha log\left(\frac{t}{t_p}\right) \tag{2.18}$$

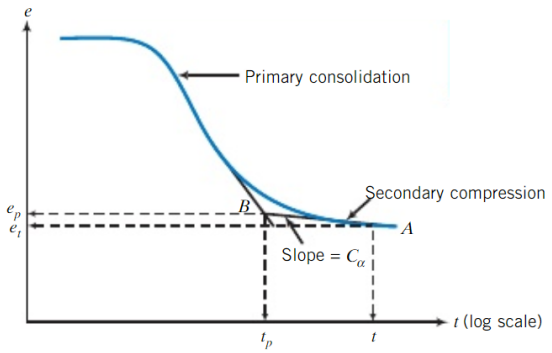

Figure 2.2: Primary consolidation and secondary compression in time
Source: Muni Budhi - Soil Mechanics and Foundations (2007)

To take into account the importance of lateral strains for the primary consolidation settlement, Skempton and Bjerrum (1957) proposed a method to modify the 1D equations. The equation they propose accounts for lateral stresses but not for lateral strains. The following equation was proposed:

$$\rho_{pc,SB} = \int_0^{H_0} m_v \Delta u dz \tag{2.19}$$

where Δu is the excess pore water pressure, so that in a saturated soil under axisymmetric loading the excess pore water pressure is:

$$\Delta u = \Delta\sigma_1\left(A + \frac{\Delta\sigma_3}{\Delta\sigma_1}(1-A)\right) \tag{2.20}$$

With $\Delta\sigma_1$ the increase in major vertical stress, $\Delta\sigma_3$ the increase in lateral principal stress and "A" an excess pore water pressure coefficient.

So by substitution we get:

$$\rho_{pc,SB} = \int_0^{H_0} m_v \Delta\sigma_1 \left(A + \frac{\Delta\sigma_3}{\Delta\sigma_1}(1-A) \right) dz = \sum (m_v \Delta\sigma_z H_0)\mu_{SB} = \sum \rho_{pc}\mu_{SB} \tag{2.21}$$

The one dimensional primary consolidation settlement taken into account the lateral stresses with neglecting the lateral strains can lead to an error of up to 20% [Budhu, 2000].

2.1.3. Bearing Capacity Shallow Foundations

Failure in the context of bearing capacity means that the ultimate net bearing capacity is exceeded, which is known as the maximum pressure that the soil can support above its current overburden pressure (q_{ult}). For dilating soils, failure corresponds to the peak shear stress. And for non-dilating soils failure corresponds to the critical state shear stress. For this reason the failure load in dilating soils will be referred to as the collapse load. Failure load will be used for non-dilating soils. Collapse means a sudden decrease in the bearing capacity of the soil. A foundation is known as shallow if the ratio of the embedment depth to the minimum plan dimension(width) is less or equal than 2.5 ($D_f/Width \leq 2.5$). The bearing capacity theory described by Terzaghi is taken from [Budhu, 2000].

The bearing capacity equation that are generally in use in engineering practice were derived using an analytical method called the limit equilibrium method. This method consists of 3 subsequent steps that need to be followed. First the selection of a plausible failure mechanism or failure surface need to be done. Then the forces acting on the failure surface needs to be determined. Lastly the static equilibrium equations are used to determine the collapse or failure load.

The most known and accepted bearing capacity theory is from Terzaghi (1943). In (1920) Prandtl showed theoretically that a wedge of material is trapped below a rigid plate when it is subjected to concentric loads, see I in figure 2.3. Terzaghi applied Prandtl's theory to a strip footing, a strip footing means that its length is much longer than its width. The theory is based on the assumption that the soil is a semi-infinite, isotropic, weightless rigid plastic material. Failure of the footing occurs by a wedge of soil below the footing pushing its way downward into the soil. The original bearing capacity equation by Terzaghi for a strip footing can be found in equation 2.22. Where c, q and γ and B are respectively the cohesion of the soil, the equivalent surcharge load at the footing base, the unit weight of the soil and the width of the footing.

$$q_{ult} = cN_c + \gamma D_f N_q + 0.5\gamma B N_\gamma \tag{2.22}$$

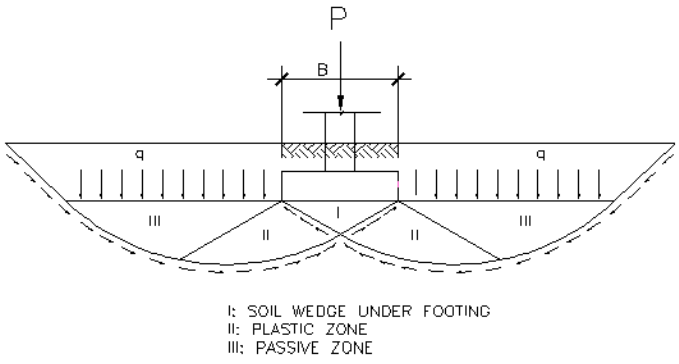

Figure 2.3: Shear failure surface assumed by Terzaghi for a strip footing

Difference is made between long-term bearing capacity (drained conditions) and short-term bearing capacity (undrained conditions). An effective stress analysis (ESA) is used for the long-term bearing capacity while a total stress analyses (TSA) is used for the short-term bearing capacity. The equations are derived for a footing at a depth D_f below the ground level of a homogeneous soil, D_f is also called embedment depth. Terzaghi assumed the following:

- The embedment depth is not greater than the width of the footing ($D_f < B$).
- General shear failure occurs (shear planes fully developed).
- The angle θ in the wedge is ϕ' (Generic friction angle).
- The shear strength of the soil above the footing base is negligible.
- The soil above the footing base can be replaced by a surcharge stress ($= \gamma D_f$).
- The base of the footing is rough.

Later Vesic found in 1973 that $\theta = 45° + \phi'/2$. Taking this into account and using the limit equilibrium analysis and modifications to take into account for the shapes of footings, the ultimate net bearing capacity equations become:

$$TSA : q_{ult} = 5.14 s_u s_c \tag{2.23}$$

$$ESA : q_{ult} = \gamma D_f (N_q - 1) s_q + 0.5 \gamma B N_\gamma s_\gamma \tag{2.24}$$

Where q_{ult} is the ultimate net bearing capacity, the ultimate pressure that the soil can support by installing a foundation above its current overburden pressure. N_q and N_γ are bearing capacity factors that are functions of the friction angle ϕ'. s_u is the undrained shear strength, s_c, s_q and s_γ are shape factors for the foundation. The bearing capacity factors are calculated as follows:

$$N_q = e^{\pi tan((\phi')} tan^2(45° + \phi'/2) \tag{2.25}$$

$$N_\gamma = 2(N_q + 1) tan(\phi') \tag{2.26}$$

The shape factors are:

$$s_c = 1 + 0.2\frac{B}{L}, \quad s_q = 1 + \frac{B}{L} tan(\phi'), \quad s_\gamma = 1 - 0.4\frac{B}{L} \tag{2.27}$$

For strip footings in equation 2.24 the ratio B/L approaches zero. A lot of adjustments and extensions are made on the Terzaghi bearing capacity formulas to get to a better approximation for different applications, but the base is always Terzaghi. Another similar approach based on Terzaghi is done by Meyerhof (1963). Meyerhof included the shearing resitance of the soil above the footing base, which means the failure surface extends to the ground surface and seems more realistic so a depth factor (d) was added. The undrained and drained equation for a vertical load are given respectively:

$$TSA : q_{ult} = 5.14 s_u s_c d_c \tag{2.28}$$

$$ESA : q_{ult} = \gamma D_f (N_q - 1) s_q d_q + 0.5 \gamma B N_\gamma s_\gamma d_\gamma \tag{2.29}$$

The corresponding shape and depth factors are given as follows:

$$s_c = 1 + 0.2\frac{B}{L}, \quad s_q = s_\gamma = 1 + 0.1 K_p \frac{B}{L} \tag{2.30}$$

$$d_c = 1 + 0.2\frac{D_f}{L}, \quad d_q = d_\gamma = 1 + 0.1\sqrt{K_p}\frac{D_f}{L} \tag{2.31}$$

$$\text{where,} \qquad K_p : tan^2\left(45° + \frac{\phi'}{2}\right) = \frac{1 + sin(\phi')}{1 - sin(\phi')} \tag{2.32}$$

All the bearing capacity equations are based on assumptions, soil variability, inaccurate soil data and uncertainties in loads. Therefore a safety factor (FS) is applied on the ultimate net bearing capacity to come to the allowable bearing capacity q_a.

$$q_a = \frac{q_{ult}}{FS} + \gamma D_f \tag{2.33}$$

2.1.4. Static and Cyclic Shear behavior of sands

In soils, the word 'strength' is often used to mean the shear strength of a soil, which is the internal frictional resistance of a soil to shearing forces. Cohesionless soils withstand shear loading through a pressure dependence friction. The shear strength of sand is quantified by the friction angle ϕ'. The shear strength of a soil represents the maximum shear stress the soil can sustain. This is represented in the Mohr-Coulomb criterion, see figure 2.4. The failure criterion is given as:

$$\tau_f = \sigma'_f tan(\phi') \tag{2.34}$$

where:

τ_f	Shear strength soil
σ'_f	Normal effective failure stress

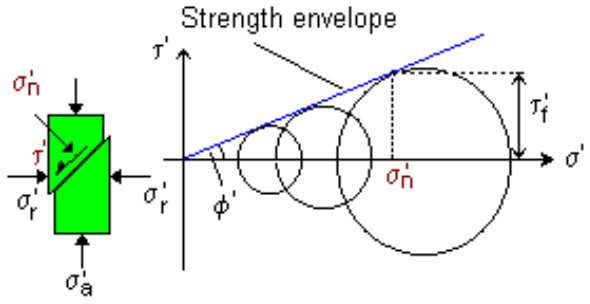

Figure 2.4: Mohr-Coulomb fialure criterion
Source: http://environment.uwe.ac.uk/geocal/SoilMech/basic

The shear behaviour of soils is characterized by volume changes. By deforming a sample under simple shear ($\varepsilon_x = \varepsilon_y = 0$) two different results can be obtained depending on the soil sample, see figure 2.5. Type I soils represents mostly loose sand and normally consolidated or lightly overconsolidated clays (OCR<2). Type II soils represent dense sand and overconsolidated clays (OCR>2). For loose sands a volume decrease is obtained (compaction), while for dense sands a volume increase (expansion) is noticed.

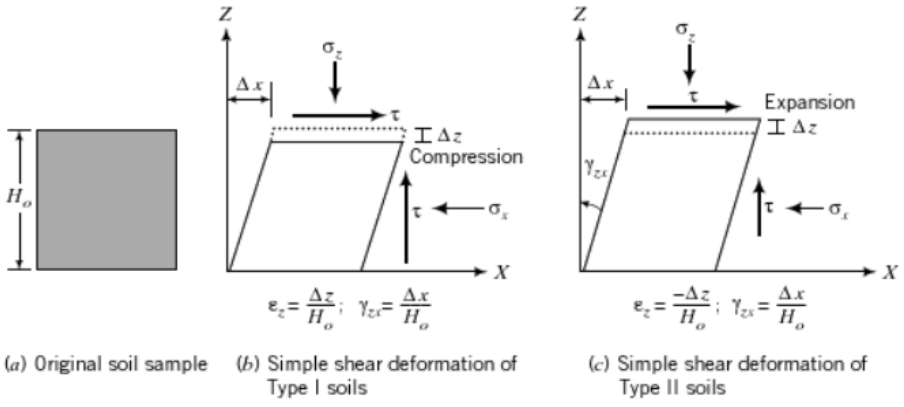

Figure 2.5: Simple shear deformation Type I (loose sand) and Type II (dense sand) soils
Source: Muni Budhu - Soil Mechanics and Foundations (2008)

Considering a constant vertical (normal) effective stress and increasing shear strain different behavior can be found, see figure 2.6. Loose sands show a gradual increase in shear stress with increasing shear strain up to an approximate constant shear stress. This shear stress is called the critical state shear

stress τ_{cs} this effect is known as strain hardening. Due to the compression the sand becomes denser until a constant void ratio is reached, the critical void ratio e_{cs}. At this state no further volume change occurs due to shearing.

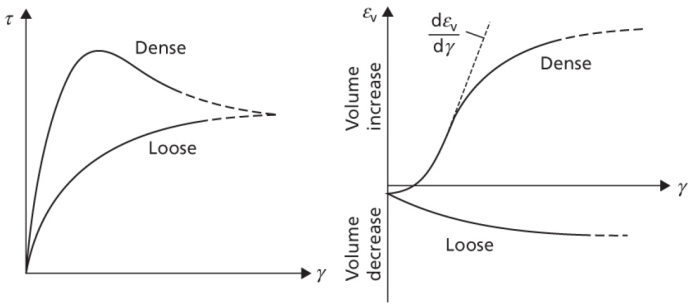

Figure 2.6: Shear strain behavior of dense and loose sand with their corresponding volume change
Source: Federico Pisano - Course: Offshore Geotechnical Engineering (Offshore soil behavior fundamentals)

In case of dense sand a rapid increase of shear stress reaching a peak value at relatively low shear strains. After the peak a decrease in shear stress with increasing shear strain up to the critical shear stress, see figure 2.6. This phenomenom is known is strain softening. Dense sands show first some contraction and then expand so the sand particles become looser. This process is known as dilation. In a dense packing shear deformation is restrained by interlocking of the particles. In order to deform the particles need to slide over each other or pushed aside which result in the expansion, see figure 2.7. The effect of an increase in normal effective stress will lead to a decrease in critical void ratio. It is known that the volumetric response of sand strongly depends on the relative density, D_r (loose or dense packed):

$$D_r = \frac{e_{max} - e}{e_{max} - e_{min}} \tag{2.35}$$

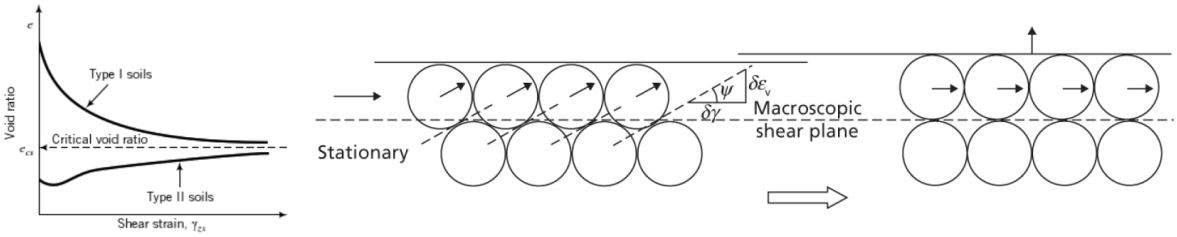

Figure 2.7: Simple shear deformation Type I and Type II soils
Source: Muni Budhu - Soil Mechanics and Foundations (2008)

Offshore structures are always subjected to wave and storm loads. Therefore the cyclic behavior of the structure and soil is of major importance. This is also the case with respect to geotechnical engineering because soil can behave significantly different under cyclic loading. Cyclic loading generates excess pore pressures, which reduce the effective stresses in the soil and causing average and cyclic shear strains to develop. This can lead to a total loss of shear strength of the soil. In the prospective of this thesis cyclic loading is in our interest because of the hammering process of the monopile. The monopile is piled into the ground by the hydraulic hammer which gives blows at different frequencies and different amplitudes.

Under undrained cyclic loading, the difference between the behavior of sands and clay is similar for many different aspects. Therefore cyclic loading for sand and clay can be dealt with in more or less the identical manner. For sands, the likelihood of liquefaction, the generated excess pore pressure due tot the loading, cyclic strains and resulting displacements and the permanent strains will be considered. The difference between drained and undrained loading is as follows:

- Drained loading: The loading is applied gradually, or the soil has a permeability that is sufficiently high, that the water flows freely out of the soil without excess pore pressures build-up. This means that all load changes are carried by the soil skeleton. This leads to soil restructuring and volume reduction.
- Undrained loading: The loading is applied rapidly, or the permeability of the soil is so low, that there is no movement of water and excess pore pressures are able to developed with respect to the steady state and lower the shear strength of the soil.

In undrained conditions excess pore pressures can affect a foundation in the following ways [Whitehouse et al., 2004]:

- Generation of net uplift pressures on the foundation
- Changes to the skin friction on the foundation wall
- Potential for seabed liquefaction

Liquefaction potential or Soil liquefaction, defined as a significant reduction in soil strength and stiffness as a result of increase in pore pressure during dynamic loading, is a major cause of damage to foundations. Liquefaction is a risk that can occur in four ways, bearing failure, settlement, localized differential lateral movements and ground loss or highly localized subsidence associated with expulsion of material. Usually in offshore applications liquefaction can occur if the following two conditions are met: a presence of loose, sandy soils or silty soils of low plasticity and a source of sudden or rapid loading, often associated with earthquakes [Malhotra, 2011]. These soil conditions are often encountered in offshore wind farm locations.

The pile installation leads to changes in soil structure and state (stresses and void ratio) in the vicinity of the foundation which affect their lateral and axial bearing capacity. This effect of pile installation is not considered in common numerical simulation methods for example with Finite Element Modelling (FEM) because these programs have difficulties with large deformations. In order to do so a new method was developed, the Material Point Method (MPM) by Sulsky [Sulsky et al., 1994]. This method can be considered as an extension of the Updated Lagrangian FEM. Where every new configuration is taken with respect to the previous configuration instead of the initial configuration and the mesh deforms as the body deforms. Recently Deltares did a study on the simulation of pile installation in saturated sand using this new MPM [Galavi et al., 2017]. The simulation was based on the six monopiles installed in Altenwalde near Cuxhaven in Germany for an extensive research program. The monopiles in Altenwalde have an outer diameter of 4.3 m, a wall thickness of 40-45 mm and a length of 21 m and were installed up to a depth of approximately 18.5 m. Three monopiles were installed with impact driving and the other three with vibratory driving. The results show that for impact pile driving some compaction of the soil occurs during pile driving and that there is pore water pressure build up at the pile toe. Under higher hammer impact for larger monopiles and with the use of an additional load of the NMS there might be some liquefaction potential.

The response of any soil to cyclic loading depends on the mode, amplitude and frequency of the loading. Where the cyclic stress, τ_{cy} and the average cyclic stress is τ_a For cyclic loading there are four different modes defined, also see figure 2.8 [Randolph and Gourvenec, 2009]:

1. Two-way cyclic loading: Cyclic loading in such a way that zero stress is crossed.
2. One-way cyclic loading: A cyclic load in a range with no zero stress level crossing.
3. Symmetric cyclic loading: A specific case of two-way loading with zero mean stress.
4. Unsymmetric cyclic loading: cyclic loading around a non-zero mean stress.

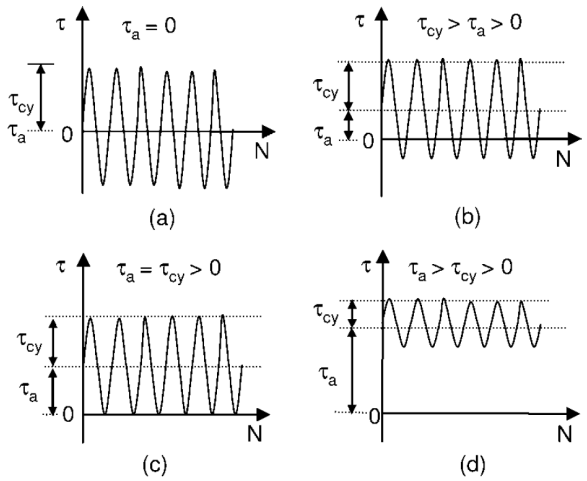

Figure 2.8: Modes of cyclic loading (a) two-way, $\tau_a = 0$ (symmetric) (b) two-way, $\tau_a > 0$ (unsymmetric) (c) one-way, $\tau_a = \tau_{cy}$ (d) one-way, $\tau_a > \tau_{cy}$
Source: Mark Randolph - Offshore Geotechnical Engineering)

The soil response is affected by the number of load cycles, the loads τ_{cy}, and τ_a and not by τ_{max}. In general for an undrained soil by increasing the number of cycles, the strain increases and the graph goes to the right. For an increasing number of cycles, the effective stress reduces due to the excess pore water pressure build up, see figure 2.9.

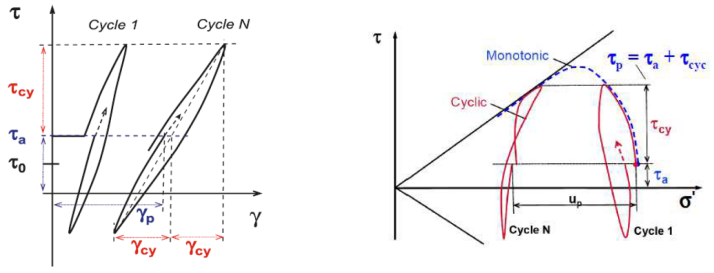

Figure 2.9: Left the stress-strain response of a soil under cyclic loading, right the corresponding stress path of the soil
Source: Federico Pisano - Course: Offshore Geotechnical Engineering (Soil behavior cyclic loading)

An example is given for a drained cyclic simple shear test on seabed sand. The sample was given a vertical and horizontal consolidated stress respectively $\sigma'_{vc} = 75kPa$ and $\sigma'_{hc} = 30kPa$. The vertical stress was maintained constant and a cyclic shear stress of $\tau_{cy} = 15kPa$ was applied during the test. Failure due to cyclic loading can occur at a lower stress than during monotonic loading. The pore pressure starts to build up leading to a reduction in vertical effective stress. Eventually when the loading continues, the excess pore pressure at the mid-point of each cycle becomes the equal to the total applied vertical load. In this case the effective stress becomes zero. The first time the effective stress falls to zero is known as the initial liquefaction. When this point is reached the sample tends to dilate with including a reduction in excess pore pressure leading to the 'butterfly' shape graph of the strain, see figure 2.10.

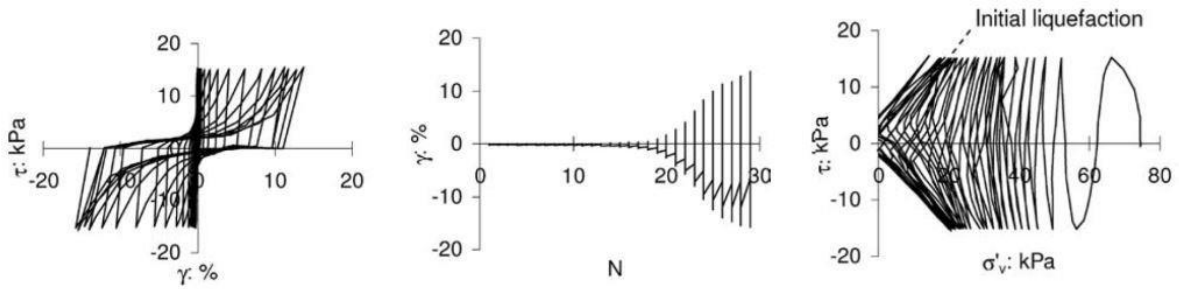

Figure 2.10: Example simple shear cyclic test
Source: Mark Randolph - Offshore Geotechnical Engineering)

A soil sample subjected to cyclic loading will develop average (u_a) and cyclic (u_{cy}) excess pore pressure and average (γ_a) and cyclic (γ_{cy}) shear strain which increase in time and the number of cycles, see figure 2.11. In case the average and or cyclic strain become very large, $\gamma_{a,cy} > 15\%$ the soil element reached failure [Andresen et al., 2011].

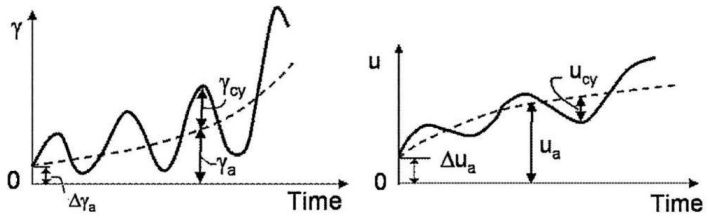

Figure 2.11: shear strain and pore pressure during cyclic loading
Source: [Andresen et al., 2011]

In order to get an overview of the effects on shear strain of the cyclic shear stress with respect to the number of cycles, the cyclic shear stress (τ_{cy}) is often normalized with the consolidation stress (sand) (σ'_{cv}) or by the monotonic consolidation stress (clays) (s_{uss}). Contour plots can be made for the strain and excess pore water pressure. In a direct shear test with a zero average shear stress. Out of the graphs in figure 2.12 the effect of the cyclic shear stress can be noticed to failure. Out of the figure it is clear that higher pore pressures are developed for a given amount of cycles (N_{cy}) at increasing ($\frac{\tau_{cy}}{\sigma'_{cv}}$). For loose sands in general, the higher $\frac{\tau_{cy}}{\sigma'_{cv}}$ the lower the amount of cycles to liquefaction.

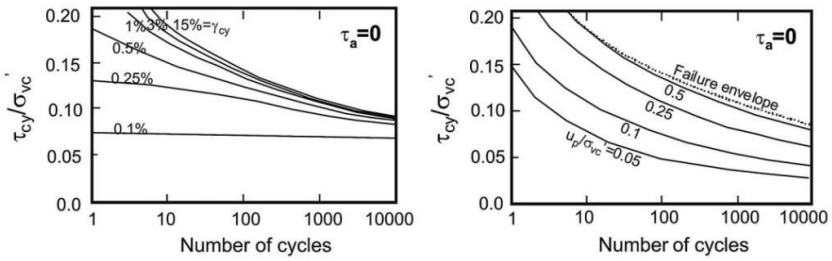

Figure 2.12: shear strain and pore pressure during cyclic loading
Source: [Andresen et al., 2011]

In fact the NMS can be seen as a shallow 'gravity based' structure. For these type of structures excluding an overturning moment the cyclic loading is likely to be one-way and compressive. The same accounts for the possible cyclic loading due to the hydraulic hammer. Keep in mind that the above theory is based on laboratory experiments and can differ from reality and the average shear stress will most probably be unequal to zero.

2.2. Scour Protection

Local scour is generally taken into account in the monopile design for offshore wind farms. Assuming a design scour depth corresponding to the most likely extreme local scour depth for both the fatigue and ultimate limit state design. Designing such a robust structure is often not technical and/or economical feasible, hence in scour prone (sandy) areas the foundations are most often designed with a scour protection system [Høgedal and Hald, 2005].

2.2.1. Occurence of Scour

Scour in the seabed occurs when waves and currents feel a transition or obstruction in the flow due to a change in the seabed profile, either a change in soil conditions or a standing structure such as a monopile can lead to scour. When a steady current encounters a monopile, the flow speeds up around the pile, producing a horse-shoe vortex, see figure 2.13. This effect amplifies the bed shear stress, if this near bed shear stress exceeds the critical near bed shear stress in the vincinity of the monopile scour occurs. This is known as clear water scour, in case the critical shear stress is exceeded everywhere on the seabed it is known as live-bed scour [Høgedal and Hald, 2005].

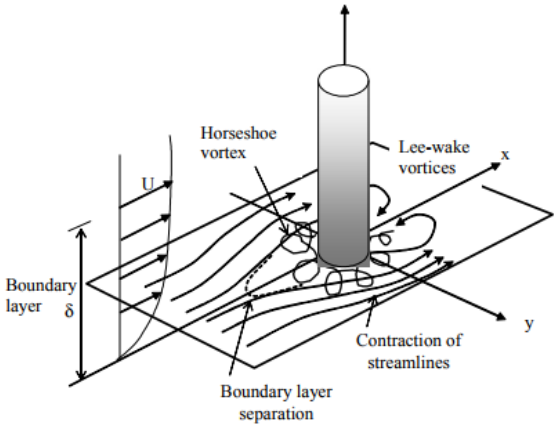

Figure 2.13: Current obstructions due to a monopile foundation in the flow, development of vortices
Source: DNVGL-ST-0126

The depth and extent of the scour mainly depends on the pile diameter D_{pile} and the current speed. We denote U_c as the depth average current speed, and the threshold value of U_c at which the sand on the undisturbed seabed starts to move as $U_{c,cr}$, the following relations are obtained [Boon et al., 2004]:

- $U_c < 0.5\ U_{c,cr}$: The bed remains stable
- $0.5\ U_{c,cr} < U_c < U_{c,cr}$: A clear water scour hole develops, which extents with increasing current velocity
- $U_c > U_{c,cr}$: A scour hole develops and the depth varies slowly with current velocity, because live-bed scour occurs and sediment is moving all over the seabed.

The effect of waves on scour is caused by the oscillatory velocities of the waves at the seabed. The scour development in the live-bed case is determined by the Keulegan-Carpenter (KC) number.

$$KC = \frac{U_m T}{D_{pile}} \tag{2.36}$$

U_m: A representative velocity amplitude of the irregular wave spectrum [m/s]

T: wave period [s]

D_{pile}: Pile diameter [m]

- KC $<$ 6, and absence of current: No scour occurs
- 6 KC $<$ 200: Scour depth and extent increase with KC
- KC $>$ 200: Scour depth and extent are equal to the steady flow case and do not depend on KC anymore.

According to [DNV.GL, 2016] in irregular waves the KC changes to:

$$KC = \frac{U_m T_p}{D_{pile}} \tag{2.37}$$

U_m: A representative velocity amplitude of the irregular wave spectrum $= 1.41 U_{rms}$ [m/s], where U_{rms} is the standard deviation of the velocity at the seabed

T_p: Peak period of the spectrum [s]

D_{pile}: Pile diameter [m]

2.2.2. Design

In 2004 Den Boon defined definitions for scour protection designs. They were named static and dynamic scour protection designs. The definitions according to Den Boon [Boon et al., 2004] are given below, for indication see figure 2.14:

Static Design: A rock armour protection layer is placed on the seabed surrounding the monopile shortly after the pile is installed. This is laid over a filter layer of finer material, placed to prevent sand being winnowed out between the rocks of the main protection layer. The filter layer is placed before installing the pile foundation.

Dynamic Design: A scour pit is allowed to develop to its equilibrium depth and extent around the monopile with no scour protection (or filter layer) in place. The scour pit is subsequently partly or wholly filled with a wide graded rock armour.

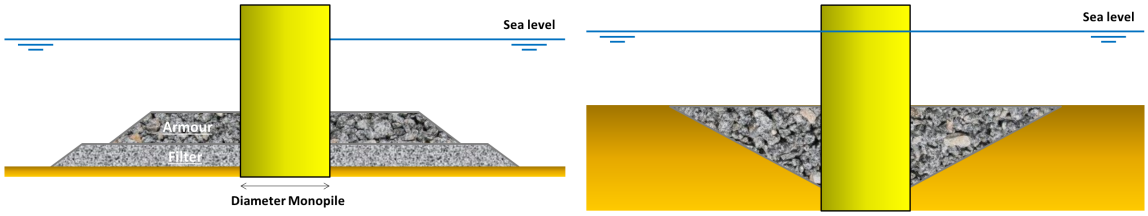

(a) Static

(b) Dynamic

Figure 2.14: Example of a static design and dynamic design according to the definition of Den Boon

The failure mechanisms for both scour protection designs are also defined by Den Boon and are quoted below [Boon et al., 2004]:

Static Design: A static protection is considered to have failed when a section of top layer armour material had disappeared completely over its full depth exposing the filter layer material over a minimum area of four armour units ($4 \cdot d_{50}^2$).

Dynamic Design: As the above definition for failure cannot be applied here (no filter layer becomes visible), it is assumed that a dynamic protection fails when a volume of rock has disappeared equal to the volume of rock that is necessary to disappear for failure of a static protection.

After Den Boon published this article back in 2004, a lot of developments have taken place. Much more wind farms are built and as knowledge develops, the use of the terms static and dynamic change as well. The current industry shows a new trend in scour protection designs, the introduction of a new dynamic scour protection. Currently three definitions will be used: static protection, dynamic protection and single layer dynamic scour protection [Willems, 2017].

Static Scour Protection: Zero movement of rocks is expected during a design storm

Dynamic Scour Protection: The dynamic protections of this time are more or less equal to the static protection that already was defined. Current dynamic protections allow deformations of the scour protection up till a certain level. Below this level scour protection as a whole is still considered not to fail. In case of a double-layer protection, failure occurs if the filter is exposed. So the definition of a static design from Den Boon is now considered as a dynamic design.

Single-layer Dynamic Scour Protection: The installed rock has 2 functions: avoid suffusion of seabed material through the scour protection and protect against waves and currents. To fulfill both functions a sufficient rock layer thickness must be applied. Therefore failure will be described based on thickness that is required to have a filter function.

In order to get a better understanding, see figure 2.15.

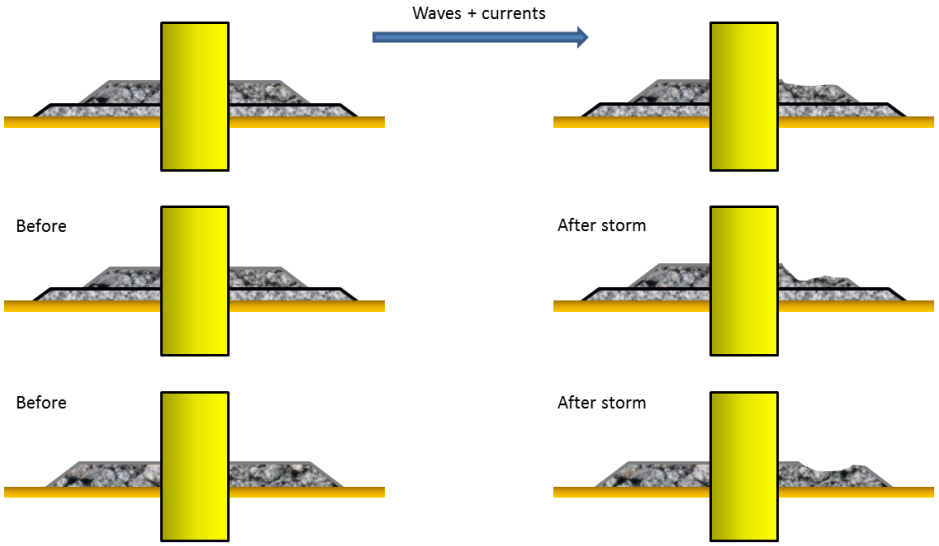

Figure 2.15: Overview of three different scour protection designs and how they deform during a design storm event. Upper figure is a static design, middle figure is a dynamic design with two layers and the bottom figure is a single layer dynamic design

Attention must be paid to the fact that scour is not prevented from occurring. Actually by installing scour protection, the scour is relocated from the monopile to the edge of the scour protection degrading the edges of the scour protection into a so called falling apron. Therefore the scour protection needs to be a certain size to have an unaffected scour protection around the monopile. In current industry a general rule of thumb of $3.5D_{pile}$ is known.

There are in principle two different scour protection designs: so called single- and multi-layer scour protection design. A multi-layer design typically exist out of two layers a so called filter which keeps the sand from washing out and an armour layer to prevent the filter from moving. For a single layer a larger rock grading and berm height is used than in the filter because it has to full fill both task at the same time. The berm need to be hydraulic stable, this means that the waves and current will not dislocate the rocks. If a filter is applied the filter needs to be stable, this means that the sand is unable to wash out. This can be calculated and is known as the static approach. For the dynamic approach, there are no known rules. Everything is based on empirical data, gathered from model tests. Out of these tests, shield parameters are determined. These parameters can be used to achieve a certain rock grading and layer thickness. The actual design of the scour protection, dimensions and rock grading(s) depend on the environmental data such as waves, current, depth and soil conditions. The scour protection will fulfill its task if the minimum berm height is maintained.

2.2.3. Stability

Input values for the stability of the scour protection are: water depth, wave height and period, current speed and direction. For calculating the stability of the rocks for the design conditions, the Shields threshold approach is used. The combined bed shear-stress τ_{cw} due to currents and waves, using the orbital velocity U_m. The Shields parameter is given as follows.

$$\Psi = \frac{\tau}{(\rho_s - \rho_w) \cdot g \cdot d_{50}} \tag{2.38}$$

Ψ: Shields parameter [-]

τ: Bed shear stress due to currents and waves $[N/m^2]$

g: Gravity acceleration (usually 9.81) $[m/s^2]$

d_{50}: Median sieve diameter of rock material $[m]$

ρ_s: Density of rock $[kg/m^3]$

ρ_w: Density of water $[kg/m^3]$

For the calculation of the bed shear stress, reference is made to [Soulsby, 1998]

$$\tau_m = \tau_c \left[1 + 1.2 \left(\frac{\tau_w}{\tau_c + \tau_w} \right)^{3.2} \right] \tag{2.39}$$

$$\tau_{max} = \sqrt{(\tau_m + \tau_w \cdot cos(\phi))^2 + (\tau_w \cdot sin(\alpha_{cw}))^2} \tag{2.40}$$

τ_c: Current only bed shear stress $[N/m^2]$

τ_w: Amplitude of oscillatory bed shear stress due to waves (H_{rms} is taken as representative wave for the full sea spectrum) $[N/m^2]$

τ_m: Mean bed shear stress during a wave cycle under combined waves and currents $[N/m^2]$

τ_{max}: Maximum bed shear stress during a wave cycle under combined waves and currents $[N/m^2]$

α_{cw}: Angle between current and wave direction [°]

A rock berm is stable, if Ψ is smaller than a certain design value, Ψ_{design}. The Shields parameter vs the dimensionless grainsize becomes constant for values larger than 200. This corresponds to grainsizes larger than 10mm. Therefore for offshore applications $\Psi_{design} = 0.055$ is often applied. So that $\Psi \leq \Psi_{design} = 0.055$.

On a sloping surface, an additional correction factor p must be applied to the design Shield parameter: $\Psi_{\alpha,design} = p \cdot \Psi_{design}$

$p = \frac{sin(\phi - \alpha)}{sin(\phi)} = cos(\alpha) \cdot \left(1 - \frac{tan(\alpha)}{tan(\phi)} \right)$

α: Angle of the slope [°]

ϕ: Natural angle of repose of the rock material (typical 40) [°]

For the layer thickness of the filter the following formula is used [Verheij et al., 2012].

$$\frac{D_F}{d_{f50}} = \frac{d_{f15}}{d_{f50}} \alpha_d ln \left(\frac{d_{f50}}{d_{b50}} \right) = 1.2 ln \left(\frac{d_{f50}}{d_{b50}} \right) \tag{2.41}$$

D_F: Filter layer thickness $[m]$

d_{f50}: Median filter diameter $[m]$

d_{b50}: Median base diameter $[m]$

α_d: Empirical coefficient (= 1.5 conservative approximation) $[-]$

For the armour layer a minimum layer thickness of $2d_{50}$ is required. There need to be at least a layer thickness of 2 stones on each other, this has also to do with the installation because it is not possible to install a smaller layer thickness. The required thickness of the single graded scour protections is mainly determined by the filter criterion. However they are mainly open filters, which means that the sediment can escape through the pores of the grading. The winnowing effect is prevented by applying a wide graded rock which reduces the openness of the protection in combination with a sufficient layer thickness of the scour protection.

2.3. Noise Mitigation

The installation of monopiles with impact pile driving produces noise. The noise is generated by impact of the hammer on the pile. The pile is deformed along the wall and the deformation is propagating down. The deformation is a consequence of the Poission effect, where a material compressed in one direction expands in another direction. Therefore the pile expands a bit in the radial direction. The sound wave travels down with a velocity $c_s = \sqrt{\frac{E}{\rho}}$, where E is the Young's modulus and ρ the density of the material. Because of the difference in travel speed in water the acoustic produced field is an axisymmetric cone. This cone is also known as the Mach cone [Reinhall and Dahl, 2011], see figure 2.16. The sound pressure level depends on the pile diameter, the soil structure and the size of the hydraulic hammer.

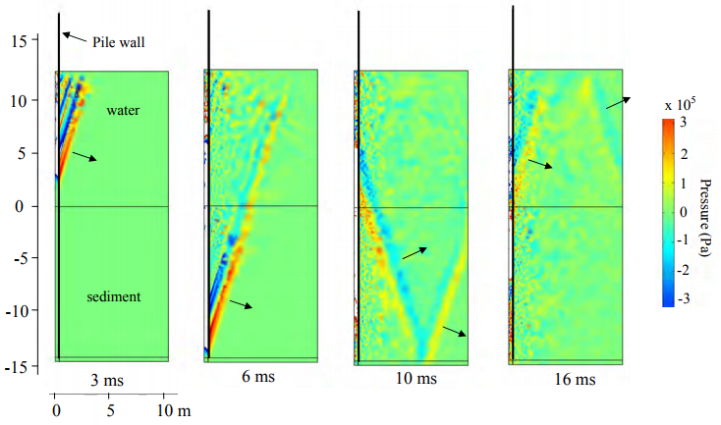

Figure 2.16: Acoustic pressure surface plots showing the acoustic radiation from the pile after 3, 6, 10, and 16 ms after impact by the pile hammer. The propagation directions of the wave fronts associated with the Mach cones produced in the water and the sediment are indicated by the arrows. are indicated by the arrows.
Source: [Reinhall and Dahl, 2011]

For all the expected windfarms in the North Sea, every country has his own noise mitigation measures. Some are with respect to noise attenuation and some have installation period restrictions and so on, an example is given for few of these measures (collected by Royal Haskoning back in 2015), see figure 2.17. For new projects also the contractors themselves can state noise regulations. All of this has lead to development of noise mitigation measures. The most common used techniques are described below and most of the information is gathered from [Koschinski and Lüdemann, 2013].

Country	Noise threshold	Noise mitigation	Seasonal restriction	Marine Mammal Detection	Marine Mammal Deterrence
Netherlands	No	No	Yes *January-July*	No	Yes *ADD and soft start*
Germany	Yes *SEL at 750 m: 160 dB* *SPL at 750 m: 190 dB*	Yes	No	No *C-PODs*	Yes *ADD and soft start*
United Kingdom	No	No	Yes *fish breeding season*	No *MMO*	Yes *ADD and soft start*
Belgium	Yes *SPL at 750 m: 185 dB*	Yes	Yes *May-August*	No	Yes *ADD and soft start*
Denmark	Yes *SEL at 750 m: 183 dB*	No	No	No	Yes *ADD and soft start*
France	No piling allowed for offshore wind farms				
Norway	No	No	No	No	No
Poland	No	No	No	No	No
Sweden	No	No	No	No	No

Figure 2.17: Example of noise regulations per country

2.3.1. Bubble Curtain

A bubble curtain is formed around a pile by bubbles that rise free to the surface by compressed air injected through a ring of perforated pipes laying at the seabed around the monopile. The radiated waves encounter a difference in density and sound velocity in the air bubbles. This leads to an impedance mismatch. The air is compressible and therefore changes the compressiblity of the water and by this the propagation velocity of the sound waves. Sound stimulation of gas bubbles near their resonance frequency effectively reduces the amplitude of the radiated sound waves by effects described by absorption and scattering. A bubble curtain is for example used by installation of Borkum West II OWF, see figure 2.18 to get an impression of the bubble curtain. Multiple rings can be used to get a better noise attenuation. There are also a lot of different configurations possible depending on the depth and environmental conditions one should decide which configuration suits the best, but one big bubble curtain seems the best solution for OWF foundations.The downside of a bubble curtain is that there is always an additional vessel required with compression packs, which is expensive. Another remark is that the working principle gets worse in case of large waves an currents which diverge the air bubbles.

(a) GeoSea vessel Goliath working with big bubble curtain for Borkum West II

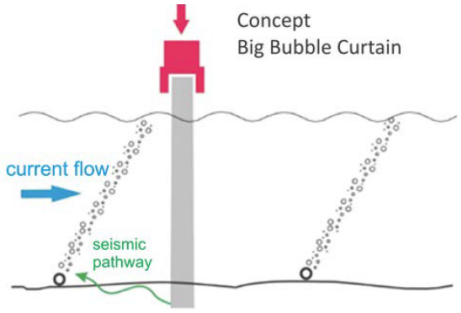

(b) Schematic view bubble curtain

Figure 2.18: Bubble Curtain overview
Source: GeoSea and Report Development of Noise Mitigation Measures in Offshore Wind Farm Construction 2013

2.3.2. Cofferdam

A cofferdam is a rigid steel tube surrounding the pile from the seabed up to the surface and there is no water in between the pile and cofferdam. Because of this pile driving takes place in air instead of water, which results in decoupling of the sound from the water body. The principle of pile in pipe piling can be used, see figure 2.19.

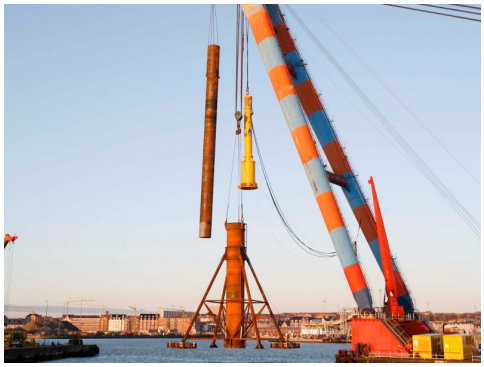

Figure 2.19: Cofferdam by Lo-Noise/SeaRenergy during test phase
Source: Nicon-Industries Esbjerg A/S

2.3.3. Hydro Sound Damper

Hydro Sound Damper (HSD) is a system with small gas filled elastic balloons and robust PE-foam elements fixed to nets or frames around the monopile. the HSD system can also be fixed to the hammer, piling frame or gripper. An example of a frame is given in figure 2.20. The efficiency of the HSD in reducing underwater noise depends on the frequency and the volume rate of the HSD. In contrast to free air bubbles of a bubble curtain, hydro sound dampers use three different physical reasons for underwater noise attenuation [Elmer and Savery, 2014].

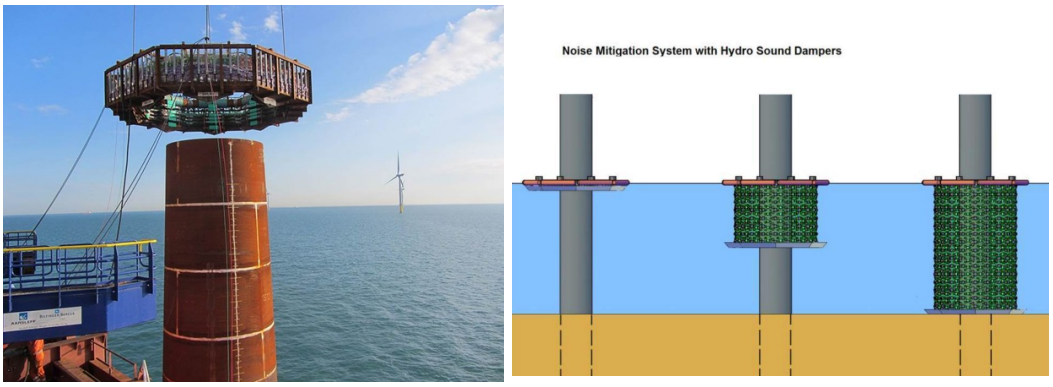

(a) Installation HSD for the London Array OWF
Source: Offshorewind.biz

(b) Schematic representation of lowering a frame HSD
Source: [Elmer and Savery, 2014]

Figure 2.20: Hydro Sound Damper

- Resonant effects of small air filled balloons and robust PE-foam elements in water can reduce the sound just as in bubble curtains. The only difference is that the resonance frequency of the HSD-elements is adjustable.
- Dissipation and material damping effects according to the material damping potential of the envelope material and the filling material inside the HSD-elements.
- Reflections of sound waves at impedance steps, because of the increased compressiblity of the mixed water-body medium.

It is also possible to fully control the HSD. The damping rate, the size, the number and distribution of the HSD around the pile are all controllable so that they can be used in the whole frequency range of pile driving noise from 50-5000 Hz.

2.3.4. Noise Mitigation Screen

A noise mitigation screen is simply said an isolation casing consisting of steel. This screen is set down around the pile reflecting a part of the noise back inside. More complex systems have additional layers containing air, foam, composites or bubbles freely rising inside. Where they make use of the impedance mismatch between water and air. Because of this absorption, scattering and dissipation effects are possible for the attenuation of the noise level. IHC Offshore Systems developed a complex Noise Mitigation System consisting of decoupled double wall isolation casing with air filled inter-space. An adjustable multi-layered bubble curtain between the pile and NMS adds an extra noise barrier. The NMS by IHC combines all the physical effects of bubble curtains, cofferdams in an isolation casing. Therefore shielding and reflection occurs from the double walled steel tube, acoustic decoupling because of the different mediums in the cofferdam and the absorption and scattering effects of the bubble curtain, see figure 2.21. Another advantage is that this system also includes a pile guiding system, which result in shorter installations times and higher workability which reduce the costs.

(a) GeoSea vessel Innovation employment of the IHC NMS-8000
Source: Royal IHC

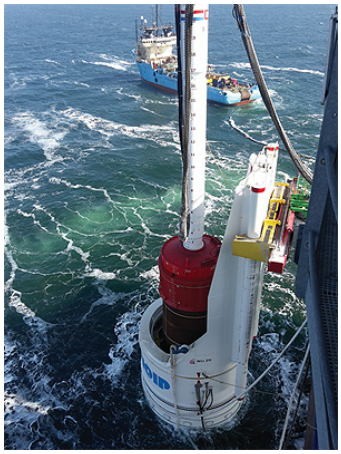

(b) Hydrohammer installing monopile through NMS
Source: Energy-oil-gas.com

Figure 2.21: IHC Noise Mitigation Screen

2.4. Installation Process

2.4.1. Monopile Foundation Installation Methods and Alternatives

Nowadays, every monopile is installed after installation of the filter layer or after installation of the total scour protection in case of a single layer system. This means that every monopile is driven through the scour protection. This section will discuss possible methods to install the monopile foundations.

Hydraulic Hammer

Most of the monopiles are installed with the use of an hydraulic hammer. IHC IQIP is the main provider of these hammers. The so called S-Series can be used above or below water in the ranges from 30-4000 kJ which corresponds to the the number behind the S. For offshore monopile installation the ranges S-1200 to S-4000 are used. The hydrohammers have an additional acceleration of the ram weight because of a Nitrogen gas spring. The operating principle is af follows. First there is a lifting phase of the ram, the pressure valve is opened and the return valve is closed. When the desired preset stroke of the ram is reached, the valves are automatically reversed. The ram starts its downward stroke where the ram is accelerated by the additional pressure of the Nitrogen gas above the piston. With this principle a maximum acceleration of 2g is reached. Because of this acceleration, the stroke that normally is required to get the same impact energy would be twice as large. So the reduction in stroke increases the blow rate of the hammer. After impact the cycle is repeated automatically. See figure 2.22 to get an impression of a hydraulic impact hammer. The power packs for the hammer are on deck of the vessel in container units.

Figure 2.22: IHC Hydrohammer S-4000 working in Galloper OWF

Vibrating Hammer

Monopiles are driven into the soil by generating vibrations in the adjecent soil particles, which reduce the resistance of the soil. The installation time of vibratory pile driving is in general shorter than in comparison with conventional impact pile driving and the noise is reduced. A vibrating low steady load at high frequency leads to low impact on the pile, so reducing the risk of fractures and fatigue. The maximum embedment depth obtainable by using vibratory pile driving depends on the soil conditions, pile diameter, wall thickness and size of the vibrating hammer. In cohesive soil, for example compact clay layers the required embedment depth can't be reached and still impact pile driving is needed to complete the task. Therefore this technique can only be used in combination with impact pile driving. APE-Holland installed the Riffgat OWF in German waters with the use of a vibratory hammer and finished the task with a smaller impact hammer, see figure 2.23.

Figure 2.23: One of Cape-Holland its Vibro hammers for the installation of the Riffgat OWF in Germany
Source: Cape-Holland

Blue Piling Technology

Blue Piling Technology is a new revolutionary technology for driving large monopiles offshore. Instead of a hydraulic impact hammer, water is used. The Blue Hammer exist of a large water tank that contains an open combustion chamber. The energy needed for the pile driving is created by gas combustion under the big water column that accelerates the water column up and down. Due to the long duration of a blow, the accelerations are relatively slow. This leads to a gradual increase of the force and reduction in noise [Fistuca, 2016]. Each phase of the piling cycle is explained in figure 2.24. The combustion under the water column leads to a pressure increase. This pressure creates an acceleration of the water in upwards direction and a downwards force that is exerted on the monopile. At the moment the water starts falling down because of the gravity another blow is delivered to the monopile which pushes the pile through the soil. The cycle is repeated after the exhaust gasses are released.

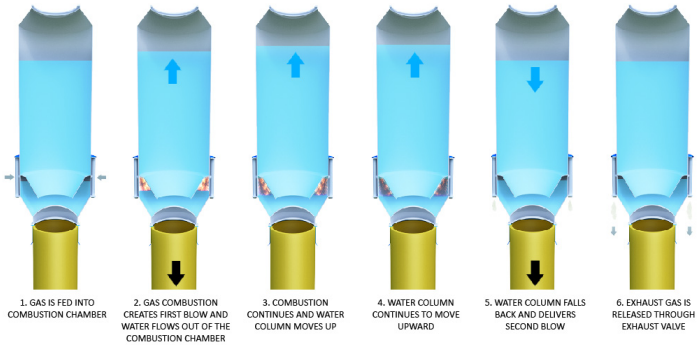

Figure 2.24: One of Cape-Holland its Vibro hammers for the installation of the Riffgat OWF in Germany
Source: Fistuca

Drilling
Drilling is also one of the options to install monopiles offshore. But in fact the so called 3D method by Fugro Seacore is used the most, 3D stands for Drive Drill Drive. So this means that nowadays impact driving is not excluded completely out of the process. First the pile is driven to its initial depth. Then the drilling equipment is set over the pile and drilling through the monopile is started. After reaching the desired drilling depth finalization is done with impact pile driving to the final elevation, see figure 2.25. This principle is for example used in Westermost Rough offshore wind farm. Located 8 kilometres off the UK's Yorkshire coast. Fugro has recently developed its biggest T120 top drill. It is the fifteenth pile top drill in the Fugro fleet and, with 120 tonnes of rotational torque, it is designed to assist in the installation of monopiles for offshore wind farm developments. The T120 is capable of drilling holes with diameters up to 8m to handle the latest XL monopiles.

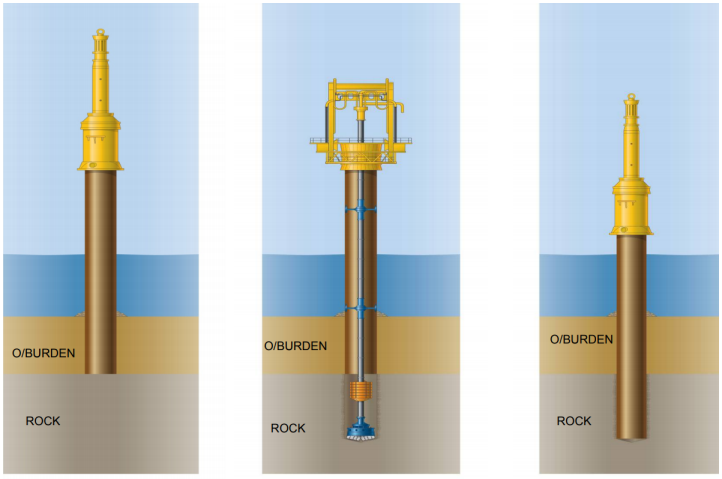

Figure 2.25: 3D monopile installation method
Source: Fugro

Gravity Based
Gravity based foundations are an alternative to monopile foundations. The grativty based foundations are installed in several offshore wind farms at relatively shallow depths. A gravity based foundation is usually a concrete based structure with or without small steel or concrete skirts. The ballast required to keep the foundation on its place consist of sand, iron ore or rock filled into the base of the structure. The structure will include a central steel or concrete shaft for the transition to the tower of the wind turbine, see figure 2.26. The base of the structure is required to be flat to ensure the upright positioning. Seabed preparations are often necessary and an additional rock blanket can be installed as a base foundation. Gravity based wind turbine foundations are usually competitive when the environmental loads are relatively modest and the ballast can be provided at low costs.

Figure 2.26: Seatower Gravity based offshore wind turbine foundation with scour protection
Source: Seatower

Suction Buckets
Bucket foundations are the other alternative for monopiles, which become more popular. Bucket foundations are buckets placed upside down into the seabed to anchor the foundation. This is done by lowering the pressure inside the bucket by pumping water out of the bucket. The created negative pressure and weight of the foundation causes the foundation to sink into the seabed. It is said that decommissioning such a structure can be done easily by reversing the process [4COffshore, 2016]. Although it has to be mentioned that bucket foundations are not applicable to all soil types. Suction buckets decrease the installation time and reduce the installation noise and weight of the structure. The biggest achievement in the offshore wind energy so far is the installation of the jacket foundation with suction buckets in the Borkum Riffgrund 1 OWF, the bucket foundation can be seen in figure 2.27.

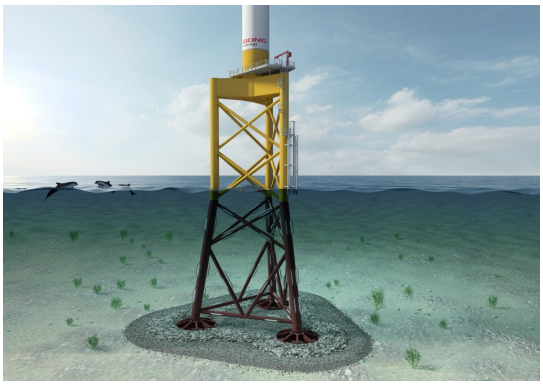

Figure 2.27: First suction bucket jacket installed in Borkom Riffgrund 1 in German water
Source: Offshorewind.biz

2.4.2. Scour Protection Installation Methods
Depending on the vessel, grading and the use of a single layer or double layer scour protection, Tideway installs the scour protection with one of the following installation methods:

- Classic Closed Fall Pipe System
- Inclined Fall Pipe System (IFPS)
- Rock Side Dump Unit (RSDU)

Classic Closed Fall Pipe System
The Fall Pipe consists of steel and/or HDPE pipe sections, allowing the length of the pipe to be adapted to the water depth. The pipe sections are stored in the Stone Dumping Unit (SDU), which is located in the center part of the vessel. This unit also contains a transport system for the pipe sections and auxiliary equipment for the pipe (dis)assembly. Furthermore, the SDU also contains hydraulic engines and winches for the suspension of the Fall Pipe and FPROV, see figure 2.28. The ROV is actively heave compensated, which provides a stable survey platform essential for the quality of data gathered by the survey sensors installed on the ROV. The FPROV will be used for pre-, intermediate- and post-surveys, but also to position the fall pipe at the correct location.

Typical characteristics of a Closed Fall Pipe system are:

- No losses of fine material due to the closed system and therefore no creation of undesired turbidity
- High production without generating uncontrolled, high flow rates at discharge end of Classic Fall Pipe.

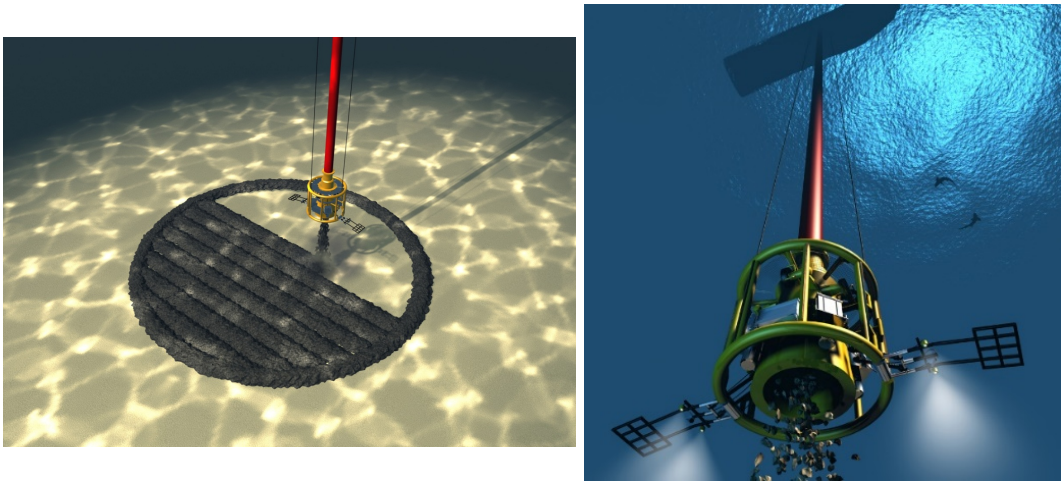

Figure 2.28: Scour protection installation with a Closed Fall Pipe System with FPROV

Inclined Fall Pipe System
For the installation of scour protection rocks close to already installed foundations the D.P. Fallpipe vessels “Tideway Rollingstone” and “Seahorse” are equipped with an inclined fallpipe system. The inclined fallpipe systems enable:

- Performance of the works with a D.P. II class vessel very close to already installed foundations.
- Accurate placement of rock to prevent any rock in possible exclusion zones.
- Controlled rock placement through Fall Pipe to ensure that no damage occurs to the foundation and possible anodes
- Installation method which ensures that segregation of the rock material during any of the steps in the installation is prevented.

The IFPS On the D.P. FPV “Tideway Rollingstone” is designed to install rocks in shallow water depths (up to 45m), close to structures such as monopiles. The system is installed on the aft of the Tideway Rollingstone where a stack of pipes (outer diameter of 1.2m) has been stored.

The IFPS consist of the following major components:

- Launcher for lowering and holding the fall pipe during operations.
- Hopper/conveyor for the rock supply, which also acts as a buffer for continued loading.
- Pipe rack for the storage of pipes.
- Pipe handling crane fixed to the aft to install and remove pipes.

The stones are transported from one of the holds over a series of conveyor belts to the aft, to be collected in the hopper. From the hopper, a final conveyor belt (used to regulate production) releases the stones above the entrance chute, see figure 2.29.

Figure 2.29: Scour protection installation with IFPS on Tideway Rollingstone
Source: Tideway

Rock Side Dump Unit
The RSDU is an over the side fall pipe system, installed on the D.P. FPV "Seahorse", capable of placing rocks up to 500kg near or around a subsea structure where a classic fall pipe system cannot be used, see figure 2.30. Typical examples are scour protection around monopiles and other offshore structures and rock berm installation in shallow waters.

Figure 2.30: Scour protection installation with RSDU on the Seahorse
Source: Tideway

The RSDU is composed out of an inclined pipe, a hopper and a bridge controlled feeder that feeds the inclined pipe with rocks discharged in the hopper by means of the on board excavator. By controlling the speed of the hopper, rocks will go through the inclined pipe with a more or less constant flow. Additionally, the system is fitted with an Obstacle Avoidance Sonar (OAS) and it is used in conjunction with a Survey Frame. Since the RSDU is positioned at the front of the vessel at port-side, rocks can be discharges only from the forward holds. In order to discharge rocks from the aft holds as well, rocks have to be transported from the aft to the front. This is done by means of the Horizontal Transport Unit (HTU).

Chapter 3

Conclusions and Recommendations

3.1. Conclusions

This thesis aims to provide a process identification regarding the impact of a NMS to the scour protection. These processes and their significant parameters are presented. Furthermore a worst case is identified in order to quantify the impact on the functionality of the scour protection. Furthermore, the worst case is evaluated based on Metocean data and validated against model tests.

A review of the available literature has been presented, providing the reader with the required knowledge regarding relevant topics such as: soil mechanics, scour protection, noise mitigation and the installation process. The research helped with understanding of the field observations and gives a first direction for the process identification.

The goal of the thesis is to evaluate the impact of the NMS on the scour protection particularly in the identified worst case. This is achieved by data analysis and the model developed to identify significant storms which have the ability to deform the scour protection.

Due to the problem's novelty, data analysis is used as a source for the process identification. The first research question revealed that the hammering process has a large influence on the NMS penetration. Similarly, the scour protection design and the actual usage of a NMS are significant factors in the deformation process. The deformation of the scour protection is only observed with the use of a NMS. Similar soil, pile, hammer and scour protection design conditions, but without using a NMS have shown no imprint in the scour protection.

One more important factor is the scour protection design. A difference is noted between the single and double layer scour protection systems. The imprint on a single layer system remains exposed to the environment, while for the double layer system the imprint in the filter is filled with the armour layer.

For the principal case analyzed the bearing capacity of the soil reveals that the soil has sufficient strength to carry the NMS load. It is concluded that the NMS penetration is mostly influenced by the dynamics of the hammer. The hammer logs revealed that more energy input during installation of the monopile leads to a larger NMS penetration. The penetration stabilizes at the moment the energy input per time becomes constant and the monopile reaches a penetration of about 15m. It is believed that this is due to the fact that the excitation energy is highest at the pile tip and the effect on the top layer is reduced. Because of the observed time-development of the deformation, and lack of liquefaction indicators, it is most likely that compaction occurred in the soil underneath the NMS, and potentially the scour protection self. Meaning the scour protection layer thickness remains intact.

The worst case is determined based on two parameters, the NMS penetration and associated mobility of the scour protection. Since the field data was limited with respect to time and storm events, significant design conditions are not met in the field. However, within the field data, a 5 year design storm was observed to occur. The chosen worst case has a mobility larger than one (1), meaning the bed shear stress induced by waves and current overcomes the critical shear stress and a NMS penetration larger than 0.5m. Due to the fact that shallower locations have a higher environmental load on the scour protection, in design phase, they are considered to be more vulnerable to deformations. Thus, the design in shallow locations is more robust, considering a HD grading. Due to lower environmental loads the deeper locations are designed with ND gradings and have higher mobility values making them a focal point in the current assessment.

The worst case is validated and evaluated against model tests. The model tests are conservative compared to the design storms. Therefore mobility values for the worst case did not meet the first 5 year test conditions. This is logical taken in to account the probability that the design storm occurred in the relative short observation period. It is concluded that less deformation occurred compared to the test. Taking into consideration hind-casting, it also means that the performance of the scour protection with NMS imprint is not affected up to these conditions. Cumulative difference plots for the worst case reveal a decrease in NMS imprint depth. This decrease is due to the fact the rocks at the edge of the imprint are most vulnerable for deformation. The monopile causes a contraction in the flow while the rock in the imprint are more sheltered. But the flow contraction has an influence zone extending outside the dimensions of the imprint. This results in a movement of the rocks towards the inside of the NMS imprint. When the scour protection has no impact from the NMS, the scour protection is loaded the most severely just around the monopile. The imprint results in a shift to the critical spot in the scour protection. The deeper the imprint, the more rock volume can be transported into it, which can lead to zones that are below the critical thickness and repairs might be necessary.

Due to the lack of available research and certain assumptions made, based on literature, this thesis has particular limitations. The findings in this thesis are only valid for scour protections around monopile foundations. The monopiles need to be installed on a sandy seabed with a loose top layer or in general German Bight conditions. Since conclusions are drawn out of hammer logs, this is only valid for pile driving with an impact hammer. The model is also based on small scour protection gradings, which means the Soulsby formula is applicable. In this thesis only one specific NMS was used in the projects. Different NMS types and other dimensions can result in a different impact on the scour protection.

Bibliography

4COffshore. Suction Bucket or Caisson Foundations, 2016. URL https://www.4coffshore.com/news/suction-bucket-or-caisson-foundations-aid11.html.

L. Andresen, H. Petter Jostad, and K. H. Andersen. Finite Element Analyses Applied in Design of Foundations and Anchors for Offshore Structures. *International Journal of Geomechanics*, 11 (6):417–430, 2011. ISSN 1532-3641. doi: 10.1061/(ASCE)GM.1943-5622.0000020. URL http://ascelibrary.org/doi/10.1061/{%}28ASCE{%}29GM.1943-5622.0000020.

J. D. Boon, J. Sutherland, and R. Whitehouse. Scour behaviour and scour protection for monopile foundations of offshore wind turbines. *... the European Wind Energy ...*, pages 1–14, 2004. URL http://scholar.google.com/scholar?hl=en{&}btnG=Search{&}q=intitle:Scour+Behaviour+and+Scour+Protection+for+Monopile+Foundations+of+Offshore+Wind+Turbines{#}0.

BSH. Offshore wind farms. Measuring instruction for underwater sound monitoring. Current approach with annotations. Application instructions. Technical report, Federal Maritime and Hydrographic Agency, 2011.

M. Budhu. *Soil Mechanics & Foundations*. John Wiley & Sons, Inc, 2000. ISBN 0-471-25231-X.

DNV.GL. DNVGL-ST-0126 : Support structures for wind turbines. *Dnv Gl As*, (April 2016), 2016.

K.-h. Elmer and J. Savery. New Hydro Sound Dampers to reduce piling underwater noise. *Internoise 2014*, pages 1–10, 2014.

W. Europe. *Deep water - The next step for offshore wind energy*. Number July. 2013. ISBN 9782930670041. URL http://www.ewea.org/fileadmin/files/library/publications/reports/Deep{_}Water.pdf.

European Commission. Directive 2009/28/EC of the European Parliament and of the Council of 23 April 2009. *Official Journal of the European Union*, 52:20, 2009. ISSN 02870827. doi: 10.3000/17252555.L_2009.140.eng.

European Parliament and the Council. Proposal for a Directive of the European Parliament and of the Council on the promotion of the use of energy from renawable resources. 0382, 2016.

EWEA. Wind energy scenarios for 2030. *Ewea*, (August):1–8, 2015. ISSN 1098-6596. doi: 10.1017/CBO9781107415324.004. URL http://www.ewea.org/fileadmin/files/library/publications/reports/EWEA-Wind-energy-scenarios-2030.pdf.

T. Fischer. Monopiles to remain dominant offshore foundation in Europe: consultant | New Energy Update, 2015. URL http://newenergyupdate.com/wind-energy-update/monopiles-remain-dominant-offshore-foundation-europe-consultant.

Fistuca. Technology – Fistuca, 2016. URL http://fistuca.com/technology/.

V. Galavi, L. Beuth, B. Zuada, and F. S. Tehrani. Numerical simulation of pile installation in saturated sand using material point method. *1st international conference on the Material Point Method*, 00 (2016):1–8, 2017.

M. Høgedal and T. Hald. Scour assessment and design for scour for monopile foundations for offshore wind turbines. *Copenhagen Offshore Wind*, 2005. URL http://wind.nrel.gov/public/SeaCon/Proceedings/Copenhagen.Offshore.Wind.2005/documents/papers/Critical{_}design{_}aspects/M.Hoegedal{_}Scour{_}assessment{_}and{_}design{_}for{_}scour.pdf.

B. N. Jones, T. S. Hillier, D. J. Partridge, and L. Fagan. Artificial Frond System for Seabed Scour Control at Wind Farm Platforms in Nantucket Sound, MAssachussetts. 44(0):1–9, 2003.

S. Koschinski and K. Lüdemann. Development of noise mitigation measures in offshore windfarm construction. *Commissioned by the Federal Agency for Nature Conservation*, (February):1–102, 2013.

S. Malhotra. Selection, Design and Construction of Offshore Wind Turbine Foundations, Wind Turbines. In *Wind turbines*, chapter 10. 2011. ISBN 978-953-307-221-0.

M. Randolph and S. Gourvenec. *Offshore Geotechnical Engineering*. Spon Press, 2009. ISBN 978-0-7277-3641-3. doi: 10.1680/ogepap.36413. URL `http://www.icevirtuallibrary.com/content/book/101130`.

P. G. Reinhall and P. H. Dahl. An Investigation of Underwater Sound Propagation from Pile Driving. *WSDOT Research Report*, page 47, 2011. URL `http://www.wsdot.wa.gov/research/reports/fullreports/781.1.pdf`.

R. Soulsby. *Dynamics of marine sands - a manual for practical applications*. Thomas Telford Publishing, 1998. ISBN 978-0727725844.

D. Sulsky, Z. Chen, and H. Schreyer. A particle method for hystory-dependent materials. *Computer Methods in Applied Mechanics and Engineering*, 118(1-2):179–196, 1994. ISSN 00457825. doi: 10.1016/0045-7825(94)90112-0.

J. van der Tempel, M. B. Zaaijer, and H. Subroto. The effects of Scour on the design of offshore wind turbines. *Proceedings of the 3rd International Conference on Marine Renewable Energy*, (2000):27–35, 2004.

H. Verheij, G. Hoffmans, K. Dorst, and S. Vandesande. Interface stability of granular filter structures under currents. *Icse6*, (1):241–248, 2012.

R. J. S. Whitehouse, S. Dunn, J. S. Alderson, and S. L. Dunn. Seabed : Scour and Liquefaction. *Proceedings of 29th International Conference on Coastal Engineering Lisbon, Portugal*, (September): 1–10, 2004.

J. Willems. Design of Scour Protection. Technical Report August, 2017.

Wind Europe. The European offshore wind industry - Key trends and statistics 2016. *Key trends and statistics 2016*, (January):33, 2017.

WindEurope. Unleashing Europe's offshore wind potential - A new resource assessment. (June), 2017a.

WindEurope. Wind energy today | WindEurope, 2017b. URL `https://windeurope.org/about-wind/wind-energy-today/`.